arXiv:1002.3834v1 [physics.data-an] 19 Feb 2010

Effects of coarse-graining on the scaling behavior of long-range correlated and anti-correlated signals

Yinlin Xu[1,2], Qianli D.Y. Ma[3,4], Daniel T. Schmitt[1], Pedro Bernaola-Galván[5] and Plamen Ch. Ivanov[1,3,5*]
[1] *Center for Polymer Studies and Department of Physics,Boston University, Boston, MA 02215, USA*
[2] *College of Physics Science and Technology, Nanjing Normal University, Nanjing 210097, China*
[3] *Harvard Medical School and Division of Sleep Medicine, Brigham & Women's Hospital, Boston, MA 02215, USA*
[4] *College of Geography and Biological Information, Nanjing University of Posts and Telecommunications, Nanjing 210003, China*
[5] *Departamento de Física Aplicada II, Universidad de Málaga, 29071 Málaga, Spain*

We investigate how various coarse-graining methods affect the scaling properties of long-range power-law correlated and anti-correlated signals, quantified by the detrended fluctuation analysis. Specifically, for coarse-graining in the magnitude of a signal, we consider (i) the Floor, (ii) the Symmetry and (iii) the Centro-Symmetry coarse-graining methods. We find, that for anti-correlated signals coarse-graining in the magnitude leads to a crossover to random behavior at large scales, and that with increasing the width of the coarse-graining partition interval Δ this crossover moves to intermediate and small scales. In contrast, the scaling of positively correlated signals is less affected by the coarse-graining, with no observable changes when $\Delta < 1$, while for $\Delta > 1$ a crossover appears at small scales and moves to intermediate and large scales with increasing Δ. For very rough coarse-graining ($\Delta > 3$) based on the Floor and Symmetry methods, the position of the crossover stabilizes, in contrast to the Centro-Symmetry method where the crossover continuously moves across scales and leads to a random behavior at all scales, thus indicating a much stronger effect of the Centro-Symmetry compared to the Floor and the Symmetry methods. For coarse-graining in time, where data points are averaged in non-overlapping time windows, we find that the scaling for both anti-correlated and positively correlated signals is practically preserved. The results of our simulations are useful for the correct interpretation of the correlation and scaling properties of symbolic sequences.

PACS numbers: 05.04.–a

I. INTRODUCTION

Certain complex physical and biological systems have no characteristic scale and exhibit long-range power-law correlations. Due to nonlinear mechanisms controlling the underlying interactions, the output signals of complex systems are also typically nonstationary, characterized by embedded trends and heterogeneous segments with different local statistical properties. Traditional methods such as power-spectrum and auto-correlation analysis [1–3] are not suitable for nonstationary signals. To address this problem, detrended fluctuation analysis (DFA) was developed to more accurately quantify long-range power-law correlations embedded in a nonstationary time series [4, 5]. In addition to quantifying scale-invariant features, DFA has been used to also detect characteristic scales in non-homogeneous signals [6, 7].

The DFA method has been successfully applied to quantify the output dynamics of various physical and biological systems including meteorology [8], climate temperature fluctuations [9–11], river flow and discharge [12, 13], economics [14–17], neural receptors in biological systems [18], DNA [4, 19–24], cardiac dynamics [25–39], and human gait [40–42]. DFA has been also utilized to identify transitions across different states of the same system characterized by different scaling behavior, e.g., the scaling exponent for heart-beat intervals discriminates between healthy and sick individuals [25], wake and sleep state [27, 31], and across different sleep stages and circadian phases [36]. Further, it has been shown that the DFA scaling exponent obtained from symbolic DNA sequences relates to the evolutionary degree of various organisms [19].

To understand the intrinsic dynamics of a given system, it is important to know how its intrinsic nature (e.g. nonstationarities) or external manipulations such as data pre-processing can affect the results. In previous studies we have investigated the effect of various data artifacts on the DFA scaling analysis of long-range power-law correlated signals. Specifically, we considered different types of nonstationarities associated with different trends present in the signal, e.g., polynomial, sinusoidal and power-law trends [43] Further, we have studied effects of nonstationarities that are often encountered in real data or result from "standard" data pre-processing approaches, e.g., signals with segments removed, signals with random spikes as well as signals with different local behavior [44]. We have also investigated the effects of linear and nonlinear filtering of signals [45] and the effects of extreme data loss [46]. Comparative studies of the performance of the DFA method and other scaling analysis methods are presented in [5, 47, 48].

*Corresponding author: plamen@buphy.bu.edu

In this paper we focus on the effect of different coarse-graining approaches on the scaling properties of correlated signals quantified by the DFA.

Coarse-graining in the magnitude of a signal. It consists of the discretization of data and is frequently imposed by the nature of the measurements, i.e., the limitations on accuracy of instruments, acquisition-data rate or even data-storage requirements. In addition, while in many situations coarse-graining is imposed by the intrinsic nature of the data, in other cases coarse-graining is applied at a latter stage in order, for example, to compute certain information theory measures derived from Shannon entropy. These functionals can be applied only to symbolic or binned time series because they take as arguments probability distributions (in practice, we never have access to the full distribution function but only to a binned version of it).

One of these functionals, especially suitable when dealing with correlations in time series, is the mutual information. It is well known that mutual information is closely related to the correlation function but, contrary to it, mutual information captures the complete dependence structure, including nonlinear correlations [49, 50]. The estimators of mutual information require the data to be binned, i.e., the range of the data is partitioned and each element of the time series is assigned to an interval of the partition. This transformation is equivalent to the coarse-graining procedures described in this study, and depending on the details of such transformation the correlation structure of the signal can be modified. For example, it is known that uniform partitions in some situations can lead to misleading results [51]. The measure of correlations using mutual information has been used in several fields: DNA sequences [52], physiological signals [53], quantum information [54], complex systems [55, 56].

Coarse graining in time (or space). It consists of substituting the values of the signal in an interval by its mean value. Again, this procedure may appear as a direct effect of the measurement (e.g. sonometers or pyranometers integrate the input during the measurement interval) or due to further modification of data. It is common to use this coarse-graining to smooth out the short scale heterogeneities of a signal. For example it has been recently used to analyze the long-scale structure of DNA [57–60]. Another typical application of coarse-graining in time is the mean-field approximation where one considers the mean effect of the interactions during a given period (in time or space) in order to simplify the problem. For example, such techniques have been used to study the growth of fractal structures in the framework of mean-field approximation [61].

The outline of this paper is as follows. In Sec. II, we review the Fourier filtering method for generating long-range power-law correlated signals and the DFA method for scaling analysis, and we introduce the Floor, Symmetry and Centro-Symmetry methods of coarse-graining in the magnitude of a signal and the coarse-graining in time method. In Sec. III we compare the scaling properties before and after coarse-graining for both anti-correlated and positively correlated signals to study the effects of various coarse-graining approaches on the DFA scaling. In Sec. IV we summarize our findings.

II. METHOD

A. Fourier filtering method

Using a modified Fourier filtering method [62], we generate stationary uncorrelated, correlated, and anti-correlated signals $x(i)$ ($i = 1, 2, 3, ..., N_{\max}$) with a zero mean and standard deviation $\sigma = 1$. This method consists of the following steps:

(a) First, we generate a random uncorrelated and Gaussian distributed sequence $\eta(i)$ and calculate the Fourier transform coefficients $\eta(q)$.

(b) The desired signal $x(i)$ must exhibit correlations, which are defined by the form of the power spectrum

$$S(q) = \langle x(q)x(-q)\rangle \sim q^{-\beta}, \tag{1}$$

where $x(q)$ are the Fourier transform coefficients of $x(i)$,β is the Fourier spectrum exponent. Thus, we generate $x(q)$ using the following transformation:

$$x(q) = [S(q)]^{1/2}\eta(q) \sim \frac{\eta(q)}{q^{\beta/2}}, \tag{2}$$

where $S(q)$ is the desired power spectrum in Eq. (1).

(c) We calculate the inverse Fourier transform of $x(q)$ to obtain $x(i)$.

Thus, the signal $x(i)$ we generate is a stationary long-range power-law correlated signal characterized by an auto-correlation function of the type

$$C(n) \equiv \langle x_i x_{i+n}\rangle_i \sim n^{-\gamma}, \tag{3}$$

where $\gamma = 1 - \beta$ is the correlation exponent [19]

For all cases of coarse-graining we investigate in our study, we always consider signals $x(i), i = 1, ..., N_{\max}$ of a fixed length $N_{\max} = 2^{17}$.

B. Coarse-graining methods

In practical applications coarse-graining is traditionally applied to the *magnitude* of a signal $x(i)$, i.e., coarse-graining (discretizing) the values which $x(i)$ can take. Alternatively, one can coarse-grain a signal *in time*, i.e., averaging the values $x(i + 1), ..., x(i + \Delta)$ of the signal within non-overlapping time intervals of size Δ. In this study we consider the most frequently used methods of coarse-graining:

1. *Coarse-graining in the magnitude* of a signal $x(i)$: (i) Floor method, (ii) Symmetry method, and (iii) Centro-Symmetry method.

2. *Coarse-graining in time* of a signal $x(i)$.

1. Coarse-graining in the magnitude

(i) *Floor method*. First, we define the width of the discretization partition interval:

$$\Delta = K \cdot \sigma, \tag{4}$$

where σ is the standard deviation of the signal $x(i)$, and the K is a real positive number. Next, the range of $x(i)$ values is partitioned into consecutive non-overlapping intervals of size Δ, starting from 0 in direction of both positive and negative values of $x(i)$ (see schematic illustration in Fig.1).

All data points in the entire signal $x(i)$, which fall into the *same* discretization partition interval, are then replaced by a symbol $\tilde{x}(i)$ corresponding to the index of the partition interval. The index of the partition interval is a positive or negative integer (Fig 1).

In the case of the *Floor coarse-graining method*, we apply the *floor rule* in order to obtain the coarse-grained symbolic sequence $\tilde{x}(i)(i = 1, ..., N_{\max})$:

$$\tilde{x}(i) \equiv \left\lfloor \frac{x(i)}{\Delta} \right\rfloor = \left\lfloor \frac{x(i)}{K \cdot \sigma} \right\rfloor, \tag{5}$$

where $\lfloor ... \rfloor$ denotes the floor function, which for any real value of the argument assigns the largest integer value less or equal to the argument. Thus, based on the floor rule we have:

(a) for positive $x(i)$ — any value $x(i) \in [0, \Delta)$ becomes $\tilde{x}(i) = 0$; any value $x(i) \in [\Delta, 2\Delta)$ becomes $\tilde{x}(i) = 1$; any value $x(i) \in [2\Delta, 3\Delta)$ becomes $\tilde{x}(i) = 2$, etc.

(b) for negative $x(i)$ — any value $x(i) \in [-\Delta, 0)$ becomes $\tilde{x}(i) = -1$; any value $x(i) \in [-2\Delta, -\Delta)$ becomes $\tilde{x}(i) = -2$, etc.

In Fig.1 we schematically demonstrate the coarse-graining in the magnitude procedure based on the Floor method.

In Fig.2 we illustrate the effect of coarse-graining in the magnitude based on the Floor method for segments of two representative signals $x(i)$: one with long-range power-law correlations and one with power-law anti-correlations. Note, that for values of the width of the partition interval $\Delta < 1$ the Floor coarse-graining leads to an expansion of the signals $\tilde{x}(i)$ along the y-axis. For $\Delta > 1$ the Floor coarse-graining effectively contracts the magnitude of the signals $\tilde{x}(i)$, leading to practically binary sequences (Fig.2). This effect appears stronger for anti-correlated signals compared to correlated signals (compare Fig.2c and Fig.2f).

(ii) *Symmetry method*. First, we define the width Δ of the discretization partition interval. Next, we partition the range of $x(i)$ values into consecutive non-overlapping partitions intervals of size Δ starting from 0 in direction of both negative and positive values of $x(i)$ (see Fig.3). Then, all data points in the entire signal $x(i)$, which fall into the *same* partition interval, are replaced by the symbol $\tilde{x}(i)$ (an integer positive or negative value) identical to the index of the partition interval (Fig.3).

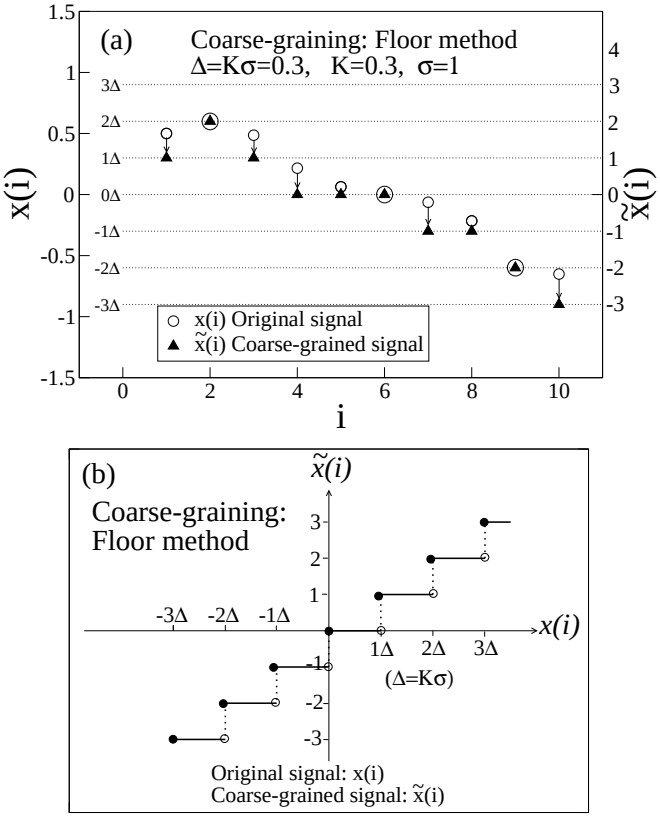

FIG. 1: Schematic illustration of the coarse-graining in magnitude procedure based on the *Floor method* (Eq. 5). (a) Coarse-graining the values of an original signal $x(i)$ (○) with a partition factor Δ to obtain a coarse-grained symbolic signal $\tilde{x}(i)$ (▲). K is the partition coefficient and σ is the standard deviation of $x(i)$. Arrows represent the shift from real values $x(i)$ to integer values (symbols) $\tilde{x}(i)$, as a result of the Floor coarse-graining. Horizontal dashed lines represent the boundaries of the discretization partition intervals. (b) Illustration of the transition from real values $x(i)$ to integer values (symbols) for the coarse-grained signal $\tilde{x}(i)$. For $x(i) < 0$ the values of $\tilde{x}(i)$ correspond to the index j of each partition interval $-j\Delta$,...,-3Δ,-2Δ,-1Δ. In contrast, for $x(i) > 0$ the values of $\tilde{x}(i)$ correspond to $(j-1)$ where j is the index of each partition interval 1Δ, 2Δ, 3Δ,...,$j\Delta$. Note, that $\tilde{x}(i) = 0$ for all values of $x(i)$ in the interval $[0, 1\Delta)$(see Eq. 5). Solid horizontal lines in (b) represent the intervals where all $x(i)$ values become coarse-grained into integers (symbols) $\tilde{x}(i)$. Open (○) and closed (●) circles indicate opened- and closed-end of the partition intervals for $x(i)$ in the Floor method transformation, e.g., all values $x(i) \in [1\Delta, 2\Delta)$ are transformed into $\tilde{x}(i) = 1$; all $x(i) \in [0, 1\Delta)$ become $\tilde{x}(i) = 0$, and all values $x(i) \in [-1\Delta, 0)$ become $\tilde{x}(i) = -1$ etc.

In the case of the Symmetry method, we apply the *symmetry rule* to obtain the coarse-grained symbolic sequence $\tilde{x}(i)(i = 1, ..., N_{\max})$:

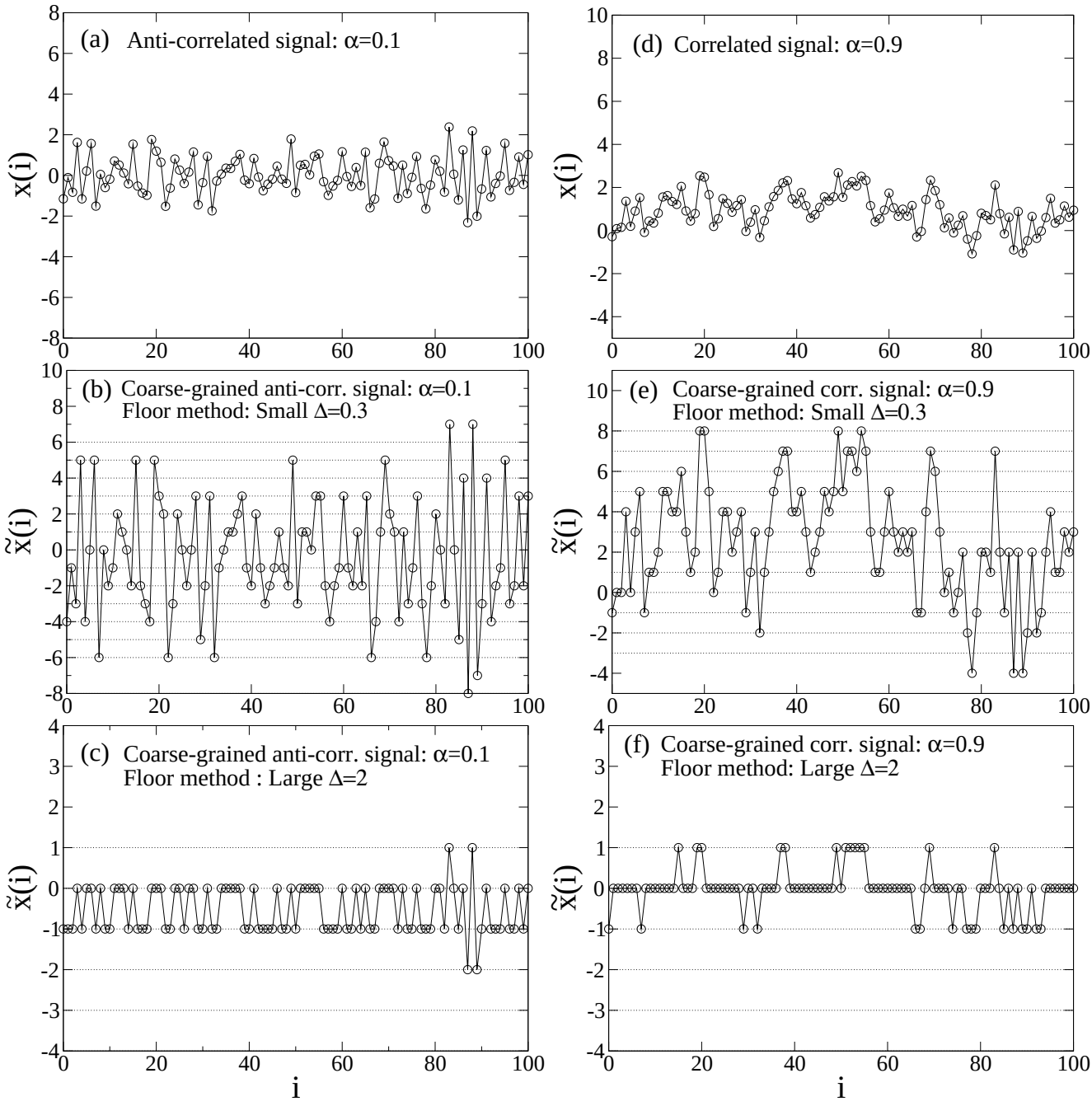

FIG. 2: Demonstration of the effect of the *Floor coarse-graining method* on (a) power-law strongly anti-correlated signal $x(i)$ characterized by a DFA scaling exponent $\alpha = 0.1$ (see Sec. II C) and (d) power-law strongly correlated signal $x(i)$ with a DFA scaling exponent $\alpha = 0.9$. Both signals in (a) and (d) have standard deviation $\sigma = 1$. For small values of the width of the discretization partition interval, $\Delta < 1$, the Floor coarse-graining method leads to expansion in the magnitude of the coarse-grained (symbolic) signal $\tilde{x}(i)$ along the y-axis with much larger standard deviation $\tilde{\sigma}$ compared to σ, shown in (b) and (e). For very large values of the width of the discretization partition interval, $\Delta \gg 1$, the Floor coarse-graining practically leads to binary sequences for both correlated and anti-correlated signals, shown in (c) and (f). We note, that for $\Delta \gg 1$ the standard deviation $\tilde{\sigma}$ of the coarse-grained signal $\tilde{x}(i)$ becomes smaller than σ of the original signal $x(i)$ (see also Fig.10 a,c).

$$\tilde{x}(i) \equiv \text{round}\left[\frac{x(i)}{\Delta} + \frac{1}{2}\text{sgn}(x(i))\right], \qquad (6)$$

where

$$\text{sgn}(x(i)) = \begin{cases} 1 & \text{if } x(i) > 0 \\ 0 & \text{if } x(i) = 0 \\ -1 & \text{if } x(i) < 0 \end{cases} .$$

The round[...] function in (6) assigns for each real argument the integer number closest to the argument. Thus based on the *symmetry rule* we have:

(a) for positive $x(i)$ — any value $x(i) \in (0, \Delta)$ becomes $\tilde{x}(i) = 1$; any value $x(i) \in [\Delta, 2\Delta)$ becomes $\tilde{x}(i) = 2$; any value $x(i) \in [2\Delta, 3\Delta)$ becomes $\tilde{x}(i) = 3$, etc.

(b) for negative $x(i)$ — any value $x(i) \in (-\Delta, 0)$ becomes $\tilde{x}(i) = -1$; any value $x(i) \in (-2\Delta, -\Delta]$ becomes $\tilde{x}(i) = -2$, etc.

(c) for $x(i) = 0$ we have $\tilde{x}(i) = 0$

In Fig.3 we schematically demonstrate the coarse-graining in the magnitude procedure based on the Symmetry method.

In Fig.4 we illustrate the effect of the coarse-graining in the magnitude of a signal based on the Symmetry method for segments of two representative signals $x(i)$: one with long-range power-law correlations and one with power-law anti-correlations. For comparison, in Fig.4 we show the same identical signal segments as shown in Fig.2. For values of the width of the partition interval $\Delta < 1$ the Symmetry coarse-graining method leads to an expansion of the signals $\tilde{x}(i)$ along the y-axis. For signal values $x(i) < 0$ the expanding effect of the Symmetry method is identical to the effect of the Floor method. However, for $x(i) > 0$ the expanding effect of the Symmetry coarse-graining method is stronger compared to the Floor method. For $\Delta > 1$ the Symmetry coarse-graining method effectively contracts the magnitude of the signals $x(i)$ leading to practically binary sequences. (see Fig.4c and Fig.4f). This effect is similar to the effect of the Floor method (compare with Fig.2c and Fig.2f).

(iii) *Centro-Symmetry method*. In contrast to the Floor and Symmetry coarse-graining methods, where the consecutive partition intervals start from 0, in the Centro-Symmetry method the first partition interval is centered at 0, i.e., $[-0.5\Delta, 0.5\Delta)$, with consecutive partitions in the positive and negative direction starting from 0.5Δ and -0.5Δ respectively.

In the case of Centro-Symmetry method we apply the *centro-symmetry* rule to obtain the coarse-grained symbolic sequence $\tilde{x}(i)(i = 1, ..., N_{\max})$:

$$\tilde{x}(i) \equiv \left\lfloor \frac{x(i) + 0.5\Delta}{\Delta} \right\rfloor, \qquad (7)$$

where $\lfloor ... \rfloor$ denotes the floor function (as in Eq.5)

Based on the Centro-symmetry rule we have:

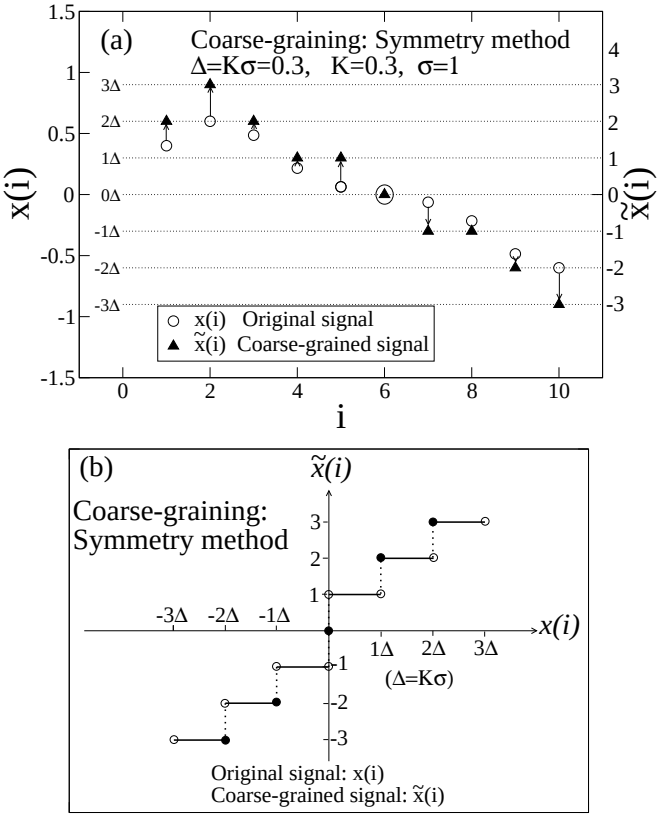

FIG. 3: Schematic illustration of the coarse-graining in magnitude procedure based on the *Symmetry method* (Eq. 6). (a) Coarse-graining the values of an original signal $x(i)$ (○) with a partition factor Δ to obtain a coarse-grained symbolic signal $\tilde{x}(i)$(▲). K is the partition coefficient and σ is the standard deviation of $x(i)$. Arrows represent the shift from real values $x(i)$ to integer values (symbols) $\tilde{x}(i)$, as a result of the Symmetry coarse-graining. Horizontal dashed lines represent the boundaries of the discretization intervals. (b) Illustration of the transition from real values $x(i)$ to integer values (symbols) for the coarse-grained signal $\tilde{x}(i)$. Note, that except for $\tilde{x}(i) = 0$, the values of $\tilde{x}(i)$ correspond to the index j of each partition interval $-j\Delta$,...,-3Δ,-2Δ,-1Δ and 1Δ,2Δ,3Δ,...,$j\Delta$ of the original signal $x(i)$ (6). For every $x(i) = 0$, after the Symmetry coarse-graining, we obtain $\tilde{x}(i) = 0$. Solid horizontal lines in (b) represent the intervals of values for $x(i)$ which become coarse-grained into integers (symbols) for $\tilde{x}(i)$. Open (○) and closed (●) circles indicate opened- and closed-end of the partition intervals for $x(i)$ in the Symmetry method transformation, e.g., all values of $x(i) \in [1\Delta, 2\Delta)$ are transformed into $\tilde{x}(i) = 2$, all values of $x(i) \in (0, 1\Delta)$ become $\tilde{x}(i) = 1$, all values of $x(i) \in (-1\Delta, 0)$ become $\tilde{x}(i) = -1$, etc.

(a) any value $x(i) \in [-0.5\Delta, +0.5\Delta)$ becomes $\tilde{x}(i) = 0$;

(b) for positive $x(i) \geq 0.5\Delta$ — any value $x(i) \in [0.5\Delta, 1.5\Delta)$ becomes $\tilde{x}(i) = 1$; any value $x(i) \in [1.5\Delta, 2.5\Delta)$ becomes $\tilde{x}(i) = 2$, etc.

(c) for negative $x(i) \leq 0.5\Delta$ — any value $x(i) \in [-1.5\Delta, 0.5\Delta)$ becomes $\tilde{x}(i) = -1$; any value $x(i) \in$

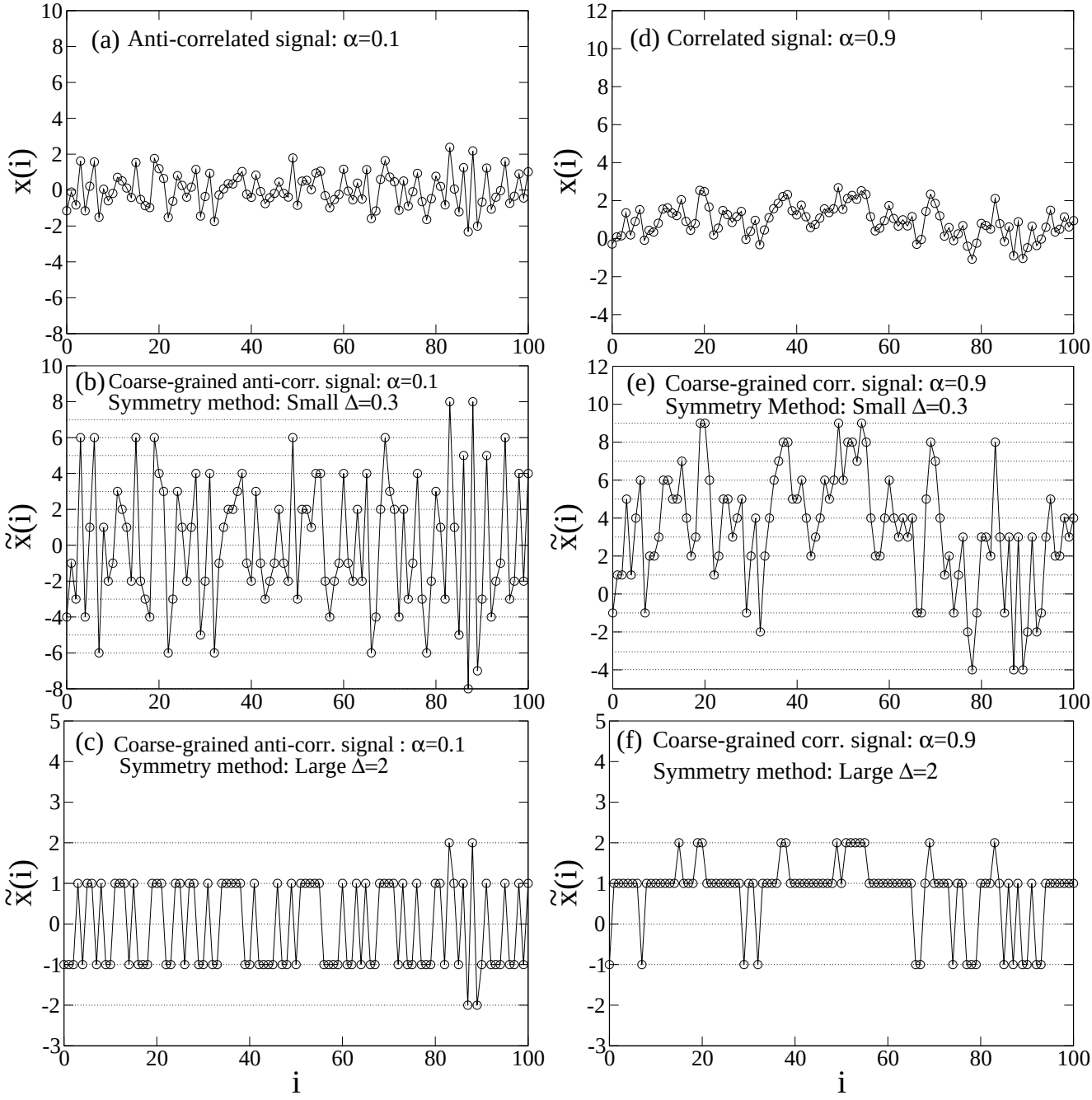

FIG. 4: Demonstration of the effect of the *Symmetry coarse-graining method* on (a) power-law strongly anti-correlated signal $x(i)$ with a DFA scaling exponent $\alpha = 0.1$ (see Sec. II C) and (d) power-law strongly correlated signal $x(i)$ with a DFA scaling exponent $\alpha = 0.9$. Both signals in (a) and (d) are identical to those shown in Fig.2a,d, and have standard deviation $\sigma = 1$. For small values of the width of the discretization interval, $\Delta < 1$, the Symmetry coarse-graining leads to expansion in magnitude of the coarse-grained symbolic signal $\tilde{x}(i)$ along the y-axis with much larger standard deviation $\tilde{\sigma}$ compared to σ, shown in (b) and (e). For very large values of the width of the partition interval, $\Delta \gg 1$, the Symmetry coarse-graining practically leads to binary sequences for both correlated and anti-correlated signals, shown in (c) and (f). We note, that for $\Delta < 1$ the expansion in magnitude of the coarse-grained signal $\tilde{x}(i)$ along the y-axis is more pronounced for the positive values of $\tilde{x}(i)$ in the Symmetry method compared to the Floor method, while for the negative values of $\tilde{x}(i)$ the magnitude expansion effect along the y-axis is the same for both Symmetry and Floor methods (compare to Fig.2b,e). We also note, that for $\Delta \gg 1$, the standard deviation $\tilde{\sigma}$ of the Symmetry coarse-grained signal $\tilde{x}(i)$ is not significantly smaller than σ of the original signal $x(i)$ (see also Fig.11 a,c). In contrast, for the Floor coarse-graining method and for $\Delta \gg 1$, $\tilde{\sigma}$ of the coarse-grained signal $\tilde{x}(i)$ is significantly smaller than σ of the original signal $x(i)$ for both correlated and anti-correlated signals (compare Fig.10 a,c to Fig.11 a,c).

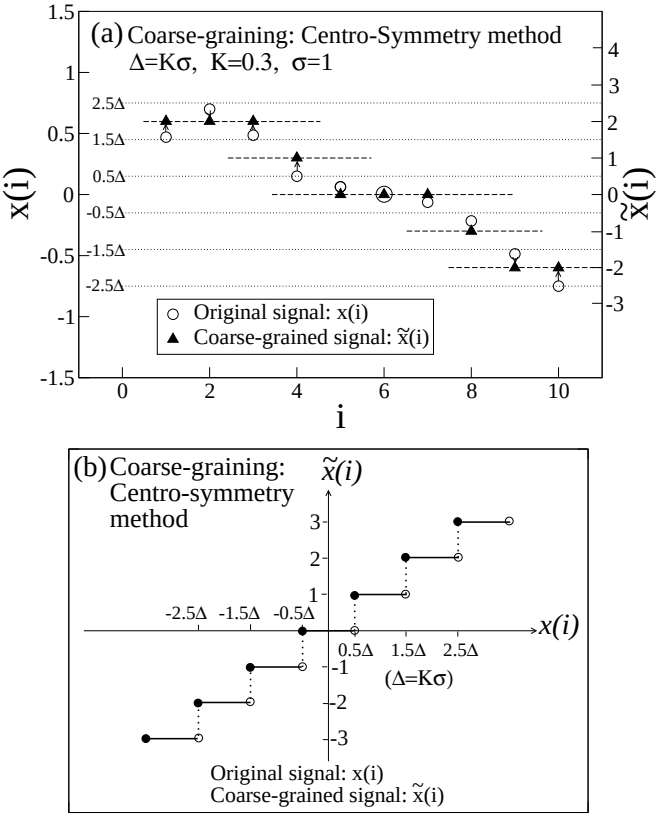

FIG. 5: Schematic illustration of the coarse-graining in the magnitude procedure based on the *Centro-symmetry method* (Eq. 7). (a) Coarse-graining the values of an original signal $x(i)$ (○) with a partition factor Δ to obtain a coarse-grained (symbolic) signal $\tilde{x}(i)$ (▲). K is the partition coefficient and σ is the standard deviation of $x(i)$. Arrows represent the shift from real values $x(i)$ to integer values (symbols) $\tilde{x}(i)$ as a result of the Centro-symmetry coarse-graining. Horizontal dashed lines represent the boundaries of the discretization intervals. Horizontal long dashed lines represent the center of each discretization interval. (b) Illustration of the transition from real values of the original signal $x(i)$ to integer values (symbols) for the Centro-symmetry coarse-grained signal $\tilde{x}(i)$. Solid horizontal lines in (b) represent the intervals of $x(i)$ values which become coarse-grained into integers (symbols) $\tilde{x}(i)$. Open (○) and closed (●) circles indicate opened- and closed-end partition intervals for $x(i)$ in the Centro-symmetry transformation, e.g., all values of $x(i) \in [0.5\Delta, 1.5\Delta)$ are transformed into $\tilde{x}(i) = 1$, all $x(i) \in [-0.5\Delta, 0.5\Delta)$ become $\tilde{x}(i) = 0$, and all values $x(i) \in [-1.5\Delta, -0.5\Delta)$ become $\tilde{x}(i) = -1$, etc.

$$[-2.5\Delta, -1.5\Delta) \text{ becomes } \tilde{x}(i) = -2, \text{ etc.}$$

In Fig.5 we schematically demonstrate the coarse-graining procedure based on the Centro-symmetry method.

In Fig.6 we illustrate the effect of the coarse graining in the magnitude based on the Centro-symmetry method for segments of two representative signals $x(i)$: one long-range power-law correlated signal and one power-law anti-correlated signal. To compare the effect of the Centro-symmetry method with the effects of the Symmetry and the Floor methods, we use in Fig.6 the same identical signal segments as in Fig.2 and Fig.4.

Note, that for values of the width of the partition intervals $\Delta < 1$, the Centro-symmetry coarse-grained signals $\tilde{x}(i)$ expand along the y-axis (Fig.6b,e), an effect similar to the Floor and Symmetry methods (Fig.2b,e and Fig.4b,e).

However, in contrast to the Symmetry method, for $\Delta > 1$ the Centro-symmetry coarse-graining leads to a relatively larger proportion of zero values for the symbolic signal $\tilde{x}(i)$ (Fig.6c,f).

2. Coarse-graining in time

In addition to coarse-graining the magnitude of a signal (as discussed in the subsection above), we also consider coarse-graining in time.

Under the coarse-graining in time procedure, we divide the signal $x(i)$ into segments corresponding to consecutive non-overlapping time intervals of size Δ, and we replace all data points in each segment by a single data point with a value equal to the average of the signal in this segment. Given a signal $x(i)(i = 1, ..., N_{\max})$, we construct a coarse-grained in time series $\tilde{x}(j)(j = 1, ..., \lfloor N_{\max}/\Delta \rfloor)$, using the following rule:

$$\tilde{x}(j) \equiv \frac{1}{\Delta} \sum_{i=(j-1)\Delta+1}^{j\Delta} x(i), \quad 1 \le j \le \left\lfloor \frac{N_{\max}}{\Delta} \right\rfloor, \qquad (8)$$

where the floor function $\lfloor N_{\max}/\Delta \rfloor$ indicates the largest integer number less or equal to $N_{\max}/\Delta$. Thus, the index j of the coarse-grained in time signal $\tilde{x}(j)$ denotes the index of the consecutive non-overlapping time intervals of size Δ which partition the original signal $x(i)$. The length of signal $\tilde{x}(j)$ is determined by the maximum number of time intervals of size Δ which can fit in the length $N_{\max}$ of the original signal $x(i)$. Thus Δ plays the role of a scale factor in 'renormalizing' (coarse-graining) the original signal.

In Fig.7 we schematically demonstrate the coarse-graining in time method. For scale factor $\Delta = 1$ the coarse-graining in time rule in Eq.8 reproduces the original signal $\tilde{x}(j) \equiv x(i)$ where j=i, i.e., coarse-graining with an unit scale factor does not coarse-grain the signal $x(i)$.

In Fig.8 we demonstrate the effect of the coarse-graining in time method for two representative signals $x(i)$: one with long-range power-law correlations and one with power-law anti-correlations. For comparison of the different coarse-graining methods, the signals we show in Fig.8 are identical to the signals shown in Fig.2, Fig.4 and Fig.6. With increasing the scale factor Δ the variability (standard deviation σ) of the coarse-grained in time signal $\tilde{x}(j)$ monotonically decreases (Fig.8). For the same value of the scale factor Δ, the reduction of variability is

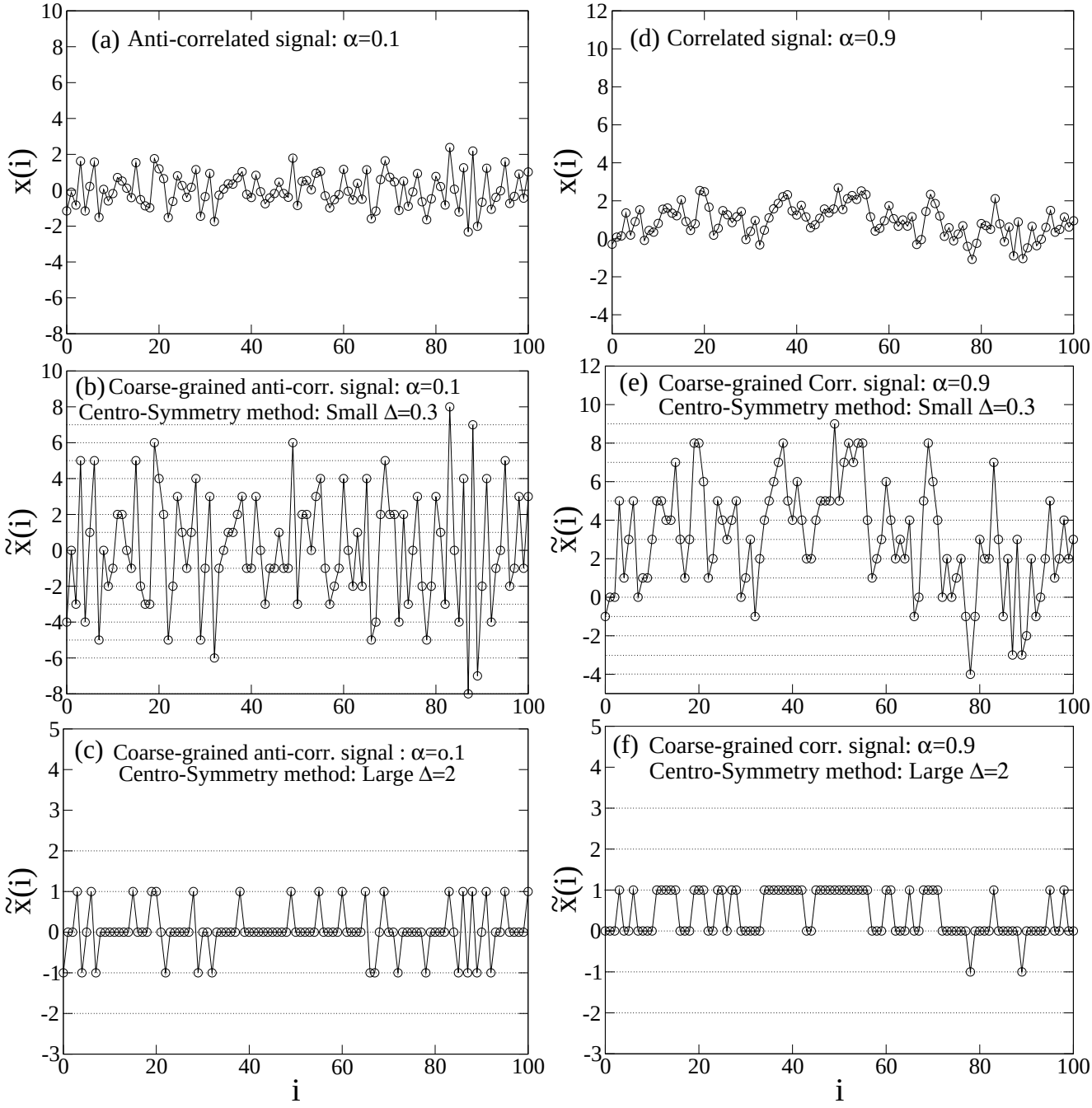

FIG. 6: Demonstration of the effect of the *Centro-symmetry coarse-graining method* on (a) power-law strongly anti-correlated signal $x(i)$ with a DFA scaling exponent $\alpha = 0.1$ (see Sec. II C) and (d) power-law strongly correlated signal $x(i)$ with a DFA scaling exponent $\alpha = 0.9$. Both signals in (a) and (d) are identical to those shown in Fig.2a,d, and Fig.4a,d, and have standard deviation $\sigma = 1$. For small values of the width of the discretization partition interval, $\Delta < 1$, the Centro-symmetry coarse-graining leads to expansion in the magnitude of the coarse-grained symbolic signal $\tilde{x}(i)$ along the y-axis with much larger standard deviation $\tilde{\sigma}$ compared to σ, shown in (b) and (e). For very large values of the width of the partition interval, $\Delta \gg 1$, the Centro-symmetry coarse-graining practically leads to binary sequences for both correlated and anti-correlated signals, shown in (c) and (f). We note that for $\Delta \gg 1$ the standard deviation $\tilde{\sigma}$ of $\tilde{x}(i)$ is significantly smaller than σ of $x(i)$ (see Fig.12a,c). We also note, that for both $\Delta < 1$ and $\Delta > 1$ the Centro-symmetry coarse-graining leads to a larger fraction of values $\tilde{x}(i) = 0$ compared to the Symmetry and Floor coarse-graining methods.

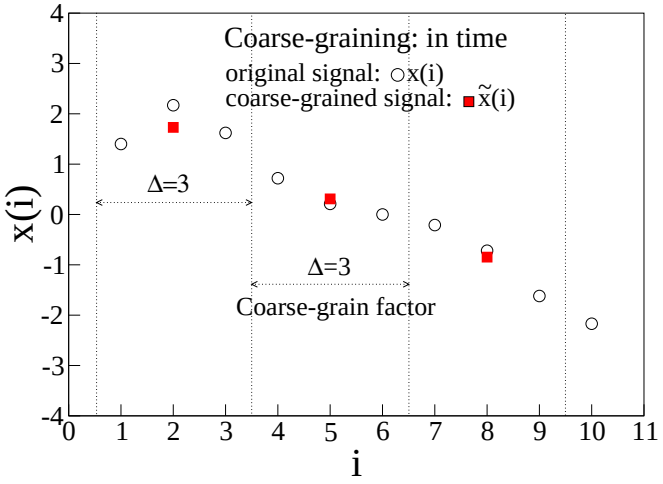

FIG. 7: Schematic illustration of the *coarse-graining in time* procedure. Coarse graining the values of an original signal $x(i)$ ($\circ$) with a scale factor (time interval) $\Delta = 3$ to obtain the coarse-grained signal $\tilde{x}(j)$ (full squares). In each time interval Δ the all values of $x(i)$ are replaced by their average $\tilde{x}(j)$ (8).

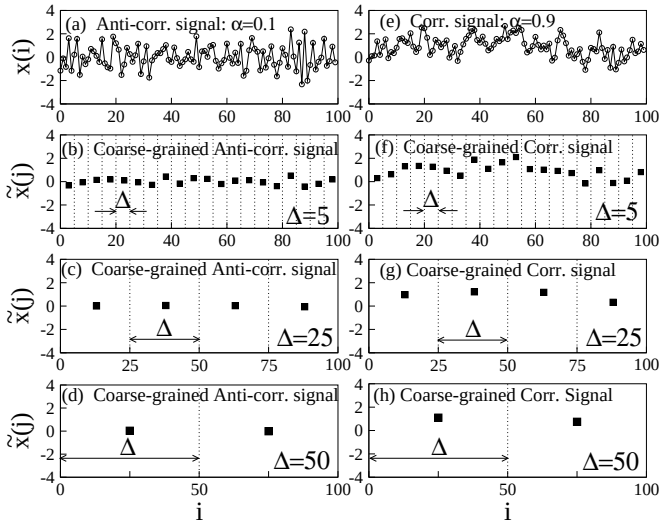

FIG. 8: Demonstration of the effect of the *coarse-graining in time* method on (a) power-law strongly anti-correlated signal $x(i)$ with a DFA scaling exponent $\alpha = 0.1$ (see Sec. II C) and (e) power-law strongly correlated signal $x(i)$ with a DFA scaling exponent $\alpha = 0.9$. Both signals in (a) and (e) are identical to those shown in Fig.2a,d, Fig.4a,d, and Fig.6a,d, and have standard deviation $\sigma = 1$. With increasing the scale factor Δ, the variability and the standard deviation is reduced for both anti-correlated (show in (b)-(d)) and for correlated signals (shown in (f)-(h)). For the same scale factor Δ, this effect is stronger for anti-correlated signals (compare (b) to (f)).

more pronounced for anti-correlated signals as compared to positively correlated signals.

C. DFA method

Using the Fourier filtering method presented in the section II A, we generate stationary signals with long-range power-law correlations. To quantify these correlations and how they change after different coarse-graining procedures, we apply the DFA method [4].

We briefly introduce the DFA method, which involves the following steps [4]:

(i) A given signal $u(i)$ ($i = 1, .., N$, where N is the length of the signal) is integrated to obtain the random walk profile $y(k) \equiv \sum_{i=1}^{k}[u(i) - \langle u \rangle]$, where $\langle u \rangle$ is the mean of $u(i)$.

(ii) The integrated signal $y(k)$ is divided into boxes of equal length n.

(iii) In each box of length n we fit $y(k)$ using a polynomial function of order ℓ which represents the *trend* in that box. The y coordinate of the fit curve in each box is denoted by $y_n(k)$. When a polynomial fit of order ℓ is used, we denote the algorithm as DFA-ℓ. Note that, due to the integration procedure in step (i), DFA-ℓ removes polynomial trends of order $\ell - 1$ in the original signal $u(i)$.

(iv) The integrated profile $y(k)$ is detrended by subtracting the local trend $y_n(k)$ in each box of length n:

$$Y(k) \equiv \; y(k) - y_n(k). \tag{9}$$

(v) For a given box length n, the root-mean-square (rms) fluctuation function for this integrated and detrended signal is calculated:

$$F(n) \equiv \sqrt{\frac{1}{N}\sum_{k=1}^{N}[Y(k)]^2}. \tag{10}$$

(vi) The above computation is repeated for a broad range of box lengths n (where n represents a specific space or time scale) to provide a relationship between $F(n)$ and n.

A power-law relation between the average root-mean-square fluctuation function $F(n)$ and the box size n indicates the presence of scaling: $F(n) \sim n^{\alpha}$. The fluctuations can be characterized by a scaling exponent α, a self-similarity parameter which represents the long-range power-law correlation properties of the signal. If $\alpha = 0.5$, there is no correlation and the signal is uncorrelated (white noise); if $\alpha < 0.5$, the signal is anti-correlated; if $\alpha > 0.5$, the signal is correlated. For stationary signals, the scaling exponent α relates linearly to the scaling exponent β of the power spectrum $S(q)$ (Eq.1) and to the correlation exponent γ of the auto-correlation function $C(n)$ (Eq.3) as:

$$\alpha = \frac{\beta + 1}{2} = \frac{2 - \gamma}{2}, \tag{11}$$

where $0 < \gamma < 1$.

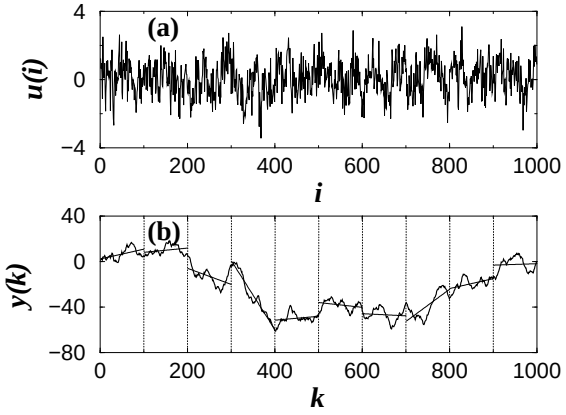

FIG. 9: (a) The correlated signal $x(i)$. (b) The integrated signal: $y(k) = \sum_{i=1}^{k}[x(i) - \langle x \rangle]$. The vertical dotted lines indicate a box of size $n = 100$, the solid straight lines segments are the estimated linear "trend" in each box by least-squares fit.

We note that for anti-correlated signals, the scaling exponent obtained from the DFA method overestimates the true correlations at small scales [43]. To avoid this problem, one needs first to integrate the original anti-correlated signal and then apply the DFA method [43]. The correct scaling exponent can thus be obtained from the relation between n and $F(n)/n$ (instead of $F(n)$). In the following sections, we first integrate the signals under consideration, then apply DFA-2 to remove linear trends in these integrated signals. In order to provide a more accurate estimate of $F(n)$, the largest box size n we use is $N_{\max}/10$, where $N_{\max}$ is the total number of points in the signal.

We compare the results of the DFA method obtained from the coarse-grained signals $\tilde{x}(i)$ with those obtained from the stationary signal $x(i)$, and examine how the scaling properties of a detrended fluctuation function $F(n)$ change when introducing different types of coarse-graining.

III. RESULTS

A. Coarse-graining in magnitude

(i) *Floor Method.* We first consider how symbolic coarse-graining in the magnitude based on the Floor method (see Section II B, Eq.5 and Fig.1) affects the scaling behavior of long-range power-law correlated signals. We systematically investigate the effect of this type of coarse-graining on both anti-correlated and correlated signals.

Anti-correlated signals: We find that the scaling behavior of anti-correlated signals is strongly affected by the Floor coarse-graining. In Fig.10(a,b,e) we present the results of Floor coarse-graining for a strongly anti-correlated signal characterized by a DFA scaling exponent $\alpha = 0.1$. For small values of the width of the partition interval $\Delta < 1$ the interface of the coarse-grained signal $\tilde{x}(i)$ expands along the y-axis, as demonstrated in Fig.2b, leading to an increase and a vertical shift up of the DFA fluctuation function $F(n)$ (Fig.10a). Further, with increasing values of $\Delta > 1$ the interface of the coarse-grained anti-correlated signal shrinks, i.e., the standard deviation decreases (as shown in Fig.2c), and the scaling curve $F(n)$ shifts vertically down (Fig.10a).

In addition, the Floor coarse-graining leads to a crossover from anti-correlated ($\alpha = 0.1$) to random behavior ($\alpha = 0.5$) in the scaling curve $F(n)$ at large scales n. This crossover is indicated by n_x in Fig.10a. With increasing values of Δ the crossover scale n_x moves from large to intermediate and small scales n. This crossover transition from large to small scales n is shown in Fig.10b where for clarity the scaling curves $F(n)$ are vertically shifted up (relative to the original signal $x(i)$ with $\alpha = 0.1$) in the order of increasing values of Δ. We note, that for very large values of Δ, the anti-correlated behavior of the original signal is not preserved even at small scales n. This crossover behavior in the scaling of anti-correlated signals reflects the different effect of the Floor coarse-graining on the temporal organization of the original signal values at large and small scales.

For fine coarse-graining with $\Delta << 1$ the relative disposition of data values in the coarse-grained signal $\tilde{x}(i)$ is preserved compared to the original anti-correlated signal $x(i)$, as shown in Fig.2a and Fig.2b. As a result, the scaling exponent α characterizing the curve $F(n)$ for $\tilde{x}(i)$ is almost the same as for the original anti-correlated signal $x(i)$ — for example, $F(n)$ for $\Delta = 0.1$ is practically parallel to $F(n)$ for the original signal except for slight deviation only at very large scales n (see Fig.10a,b). For anti-correlated signals, increasing the width of the partition interval Δ leads to stronger coarse-graining effect at larger scales while at small time scales, the relative disposition of neighboring coarse-grained data values $\tilde{x}(i)$ is preserved similar to the disposition of the corresponding original values $x(i)$, so that at small and intermediate scales the anti-correlations are preserved. Thus, the Floor coarse-graining method leads to a systematic change in the correlation properties of the original signal $x(i)$, with a crossover from anti-correlated behavior (characterized by exponent $\alpha < 0.5$) to random behavior (with $\alpha = 0.5$), and with a crossover scale n_x shifting from large to intermediate and small scales n as Δ increases.

For very rough coarse-graining, with partition parameter $\Delta \geqslant 3$, we find that even at small scales the original anti-correlated behavior is not preserved and the exponent $\alpha = 0.1$ can not be recovered (see Fig.10b). We note that because the original signal $x(i)$ has a standard deviation $\sigma = 1$, using a partition parameter $\Delta \geqslant 3$ leads practically to a binary signal $\tilde{x}(i)$ (see Fig.2c). Thus, for $\Delta > 3$ the scaling curve $F(n)$ does not change any more and remains the same as for $\Delta = 3$ (the crossover scale

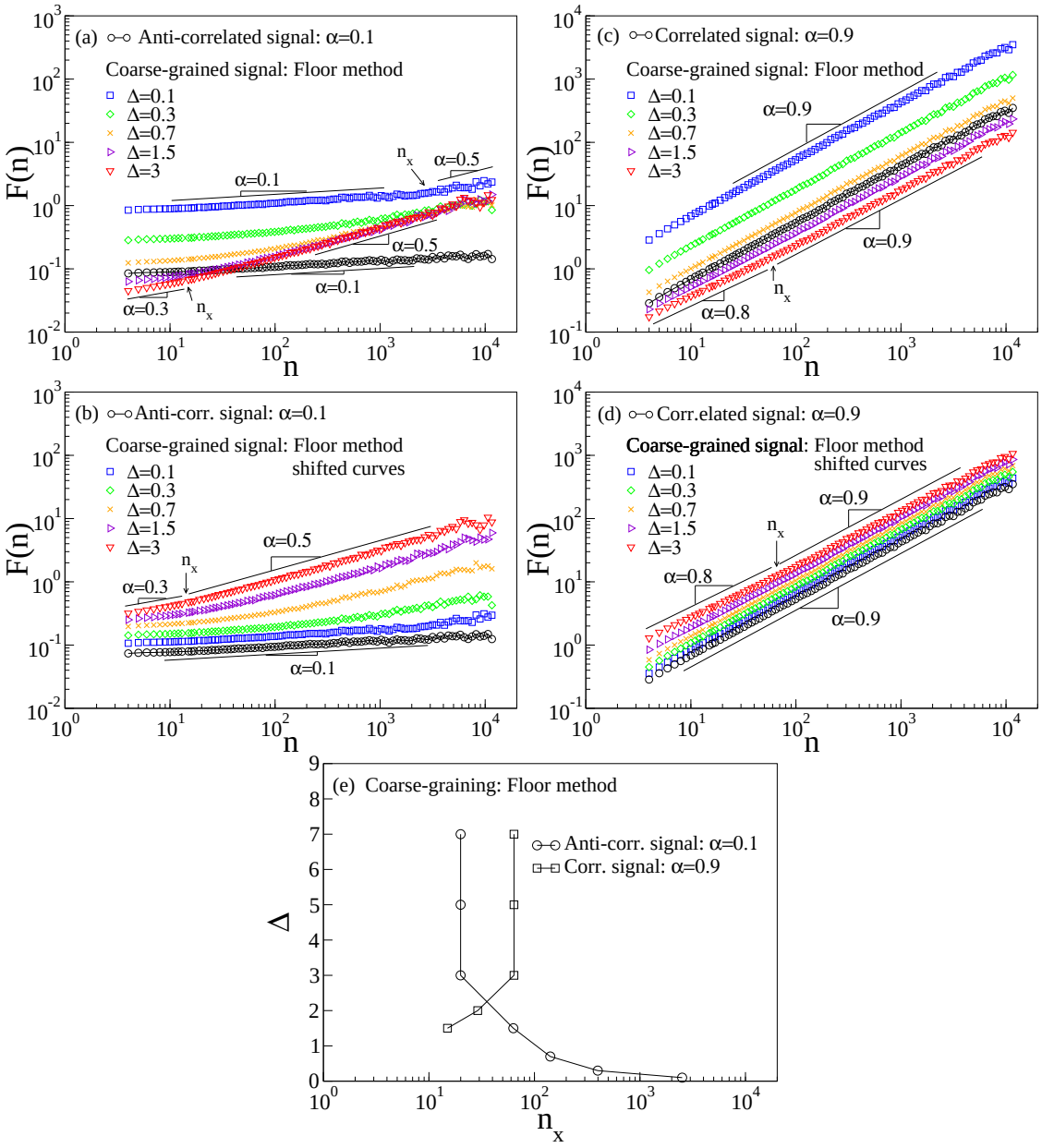

FIG. 10: Effect of the *Floor coarse-graining method* on the scaling behavior of long-range power-law correlated signals. Scaling curves $F(n)$ obtained using the DFA-2 method of (a) an anti-correlated signal with scaling exponent $\alpha = 0.1$, and (c) a positively correlated signal with $\alpha = 0.9$ before and after coarse-graining with different values of the partition parameter Δ. The same signals as shown in Fig.2a, d are used for the analysis. For $\Delta < 1$, the scaling curves $F(n)$ of the coarse-grained signals $\tilde{x}(i)$ shift up compared to $F(n)$ of the original signal $x(i)$ due to the expansion of the interface of $\tilde{x}(i)$ compared to $x(i)$ (shown in Fig.2b, e). With increasing $\Delta > 1$, the interface of $\tilde{x}(i)$ shrinks and $F(n)$ shifts down. For the anti-correlated signal in (a), the Floor coarse-graining leads to a crossover from anti-correlated ($\alpha = 0.1$) to random behavior ($\alpha = 0.5$) at a crossover scale n_x. For $\Delta < 1$ the crossover n_x corresponds to large scales, and moves to intermediate and small scales with increasing Δ. In contrast to anti-correlated signals, the Floor coarse-graining with small $\Delta < 1$ has no effect on the scaling of positively correlated signals, while for large $\Delta > 1$ there is a crossover at small scales to weaker correlations ($\alpha = 0.8$). (b) and (d) show the same results as in (a) and (c) with scaling curves $F(n)$ vertically shifted to visualize the transition of the crossover n_x for different values of Δ. We determine the crossover scale n_x based on the difference $\epsilon(n) = \log_{10}F(n) - \log_{10}F_{\rm fit}(n)$ between the scaling curve $F(n)$ of the coarse-grained signal and the linear fitting line $F_{\rm fit}(n)$ for the range of scales not affected by the coarse-graining: we chose n_x as the scale where $\epsilon(n) = 0.04$. Dependence of the crossover scale n_x on the coarse-graining parameter Δ for the anti-correlated and positively correlated signals shown in (a) and (c). Note, that for very rough Floor coarse-graining with $\Delta \geq 3$, the crossover scale n_x does not change for both anti-correlated and positively correlated signals.

n_x also does not change for $\Delta \geqslant 3$, see Fig.10(e)).

The change we observe in the scaling behavior of power-law anti-correlated signals $x(i)$ after Floor coarse-graining is similar to the effect of adding noise to each data point in $x(i)$ or of adding a percentage of random spikes of a given amplitude to the original signal. It was previously reported that random spikes alter the scaling curve $F(n)$ of an anti-correlated signal leading to a crossover from anti-correlated ($\alpha < 0.5$) behavior to random behavior ($\alpha = 0.5$) [44]. It was also reported that with increasing the amplitude of the spikes and their concentration in the original signal the crossover scale n_x gradually moves from large to intermediate and small scales (see Fig.3d in [44]), an effect identical to our results shown in Fig.10a,b. Indeed, with increasing the partition parameter Δ the difference between the values $x(i)$ in the original anti-correlated signal and the corresponding integer (symbolic) values $\tilde{x}(i)$ in the coarse-grained signal also increases, effectively equivalent to adding random noise. The rougher the coarse-graining (i.e., larger Δ) the higher the percentage and amplitude of the effectively added noise, as more data points in the original signal $x(i)$ are affected by the coarse-graining procedure (higher percentage), while at the same time the change in the relative (compared to the standard deviation of the signal) increments in $x(i)$ values is larger with increasing Δ. Thus, the effect of Floor coarse-graining on the scaling of anti-correlated signals is equivalent to a superposition of the scaling curve $F(n)$ of the original signal with the scaling curve $F_\eta(n)$ of a white noise signal ($\alpha = 0.5$). Increasing the amplitude and standard deviation of the added white noise signal leads to an increase (a vertical shift up) in $F_\eta(n)$, and thus, a shift of the intersection (i.e., the crossover scale n_x) between the $F(n)$ curves of the white noise and of the anti-correlated signal from large to smaller scales n. The role of such a superposition rule on the crossover behavior of correlated signals with nonstationarities has been discussed in detail in [43, 44].

Correlated signals: We find that the scaling behavior of positively correlated signals is much less affected by the Floor coarse-graining compared to anti-correlated signals. In Fig.10(c,d,e) we present the results for a strongly correlated signal characterized by a DFA scaling exponent $\alpha = 0.9$. For small values of the width of the partition interval $\Delta < 1$ the interface of the coarse-grained signal $\tilde{x}(i)$ expands along the y-axis, as demonstrated in Fig.2e, leading to an increase and a vertical shift up of the DFA fluctuation function $F(n)$ (Fig.10c). Further, with increasing values of $\Delta > 1$ the interface of the coarse-grained correlated signal shrinks, i.e., the standard deviation decreases (as shown in Fig.2f), and the scaling curve $F(n)$ shifts vertically down (Fig.10c). This coarse-graining effect is very similar in both positively correlated and anti-correlated signals (compare Fig.10a and Fig.10c).

In contrast to anti-correlated signals, the Floor coarse-graining with small values of the width of the partition interval $\Delta < 1$ does not affect the scaling behavior of positively correlated signals and the DFA exponent α remains unchanged at both small and large scales n, i.e., no crossover in $F(n)$ is observed (Fig.10c,d). However, for values of the partition parameter $\Delta > 1$, the Floor coarse-graining leads to a crossover in the scaling curve $F(n)$ to slightly weaker correlations (decreased scaling exponent α) at small scales n, whereas the scaling behavior at large scales remains unchanged. This crossover is indicated by n_x in Fig.10c. With increasing $\Delta > 1$, the crossover scale n_x moves from small to intermediate scales n. This crossover transition from small to intermediate scales n is shown in Fig.10d where for clarity the scaling curves $F(n)$ are vertically shifted up, relative to the original signal $x(i)$ with $\alpha = 0.9$, in the order of increasing values of Δ. We note, that even for large $\Delta \geq 3$, the scaling exponent of the Floor coarse-grained signal $\tilde{x}(i)$ at small scales decreases only slightly to $\alpha = 0.8$ from the value $\alpha = 0.9$ for the original signal $x(i)$, indicating a much weaker effect of the Floor coarse-graining on positively correlated signals compared to anti-correlated signals.

For fine coarse-graining with $\Delta < 1$ the relative disposition of data values in the coarse-grained signal $\tilde{x}(i)$ is preserved compared to the original correlated signal $x(i)$, as shown in Fig.2d and Fig.2e. As a result, the scaling exponent α for $\tilde{x}(i)$ remains unchanged — the scaling curve $F(n)$ for $\Delta = 0.1$, 0.3 and 0.7 remain parallel to $F(n)$ for the original signal $x(i)$ (see Fig.10d). Increasing the width of the partition interval $\Delta > 1$ leads to a stronger coarse-graining effect at small and intermediate scales n in contrast to anti-correlated signals where large and intermediate scales are affected.

For very rough coarse-graining, with partition parameter $\Delta \geq 3$, we find that the crossover scale n_x does not extend to large scales n and remains practically constant at $n_x \approx 60$, and at scales $n > 60$ the scaling exponent α is not affected by the Floor coarse-graining (Fig.10e). This is in contrast to anti-correlated signals where Floor coarse-graining with $\Delta \geq 3$ affects all scales (Fig.10b and Fig.10e). In Fig.10e, we summarize our findings for the effect of the Floor coarse-graining on the position of the crossover n_x for both correlated and anti-correlated signals. Specifically, we find that for anti-correlated signals n_x moves from large to small scales with increasing Δ, practically affecting the entire scaling. In contrast, for positively correlated signals a crossover to weaker correlations appears only for $\Delta > 1$ at small scales n_x, while the scaling behavior at intermediate and large scales remains unaffected. We note that for very rough coarse-graining with $\Delta \geq 3$ the crossover scale n_x remains constant for both anti-correlated and positively correlated signals.

The change we observe in the scaling behavior of power-law positively correlated signals $x(i)$ after Floor coarse-graining is similar to the effect of adding noise to each data point in $x(i)$ or of adding a percentage of random spikes of a given amplitude to the original signal. It was previously demonstrated that adding ran-

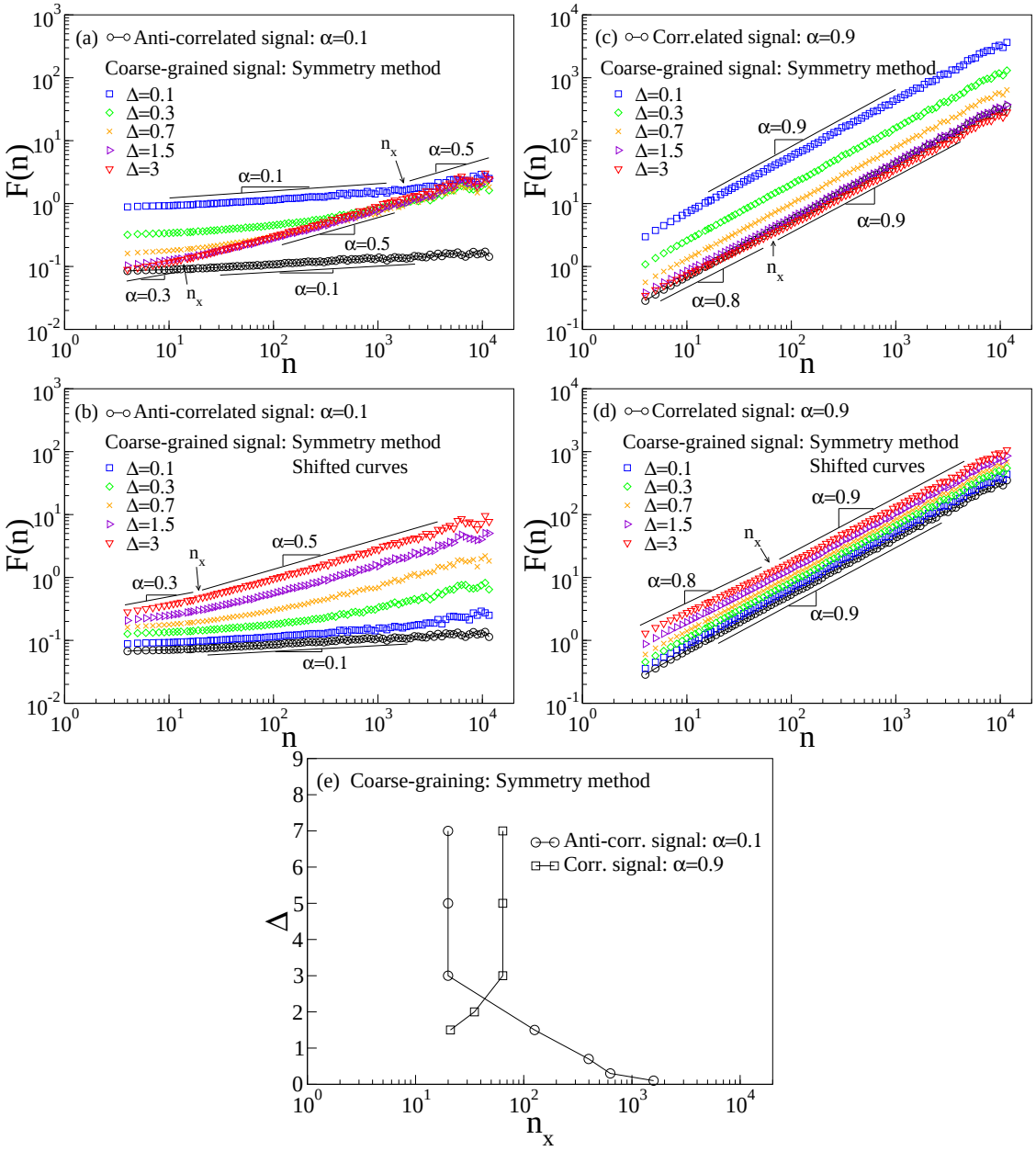

FIG. 11: Effect of the *Symmetry coarse-graining method* on the scaling behavior of long-range power-law correlated signals. Scaling curves $F(n)$ obtained using the DFA-2 method of (a) an anti-correlated signal with scaling exponent $\alpha = 0.1$, and (c) a positively correlated signal with $\alpha = 0.9$ before and after coarse-graining with different values of the partition parameter Δ. The same signals as shown in Fig.4a, d are used for the analysis. For $\Delta < 1$, the scaling curves $F(n)$ of the coarse-grained signals $\tilde{x}(i)$ shift up compared to $F(n)$ of the original signal $x(i)$ due to the expansion of the interface of $\tilde{x}(i)$ compared to $x(i)$ (shown in Fig.4b, e). With increasing $\Delta > 1$, the interface of $\tilde{x}(i)$ shrinks and $F(n)$ shifts down. Note, that for $\Delta > 1$ the scaling curves $F(n)$ of the Symmetry coarse-grained signals remain above the $F(n)$ curves of the corresponding original signals, in contrast to the effect of the Floor method where $F(n)$ of the Floor coarse-grained signals shifts below $F(n)$ of the original signals. For the anti-correlated signal in (a), the Symmetry coarse-graining leads to a crossover from anti-correlated ($\alpha = 0.1$) to random behavior ($\alpha = 0.5$) at a crossover scale n_x. For $\Delta < 1$ the crossover n_x corresponds to large scales, and moves to intermediate and small scales with increasing Δ. In contrast to anti-correlated signals, the Symmetry coarse-graining with small $\Delta < 1$ has no effect on the scaling of positively correlated signals, while for large $\Delta > 1$ there is a crossover at small scales to weaker correlations ($\alpha = 0.8$). (b) and (d) show the same results as in (a) and (c) with scaling curves $F(n)$ vertically shifted to visualize the transition of the crossover n_x for different values of Δ. (e) Dependence of the crossover scale n_x on the coarse-graining parameter Δ for the anti-correlated and positively correlated signal shown in (a) and (c). For very rough Symmetry coarse-graining with $\Delta \geq 3$, the crossover scale n_x does not change for both anti-correlated and positively correlated signals. The effect of the Symmetry coarse-graining method on the scaling of correlated and anti-correlated signals is very similar to that of the Floor method (compare with Fig.10).

dom spikes an anti-correlated signal alters the scaling curve $F(n)$ leading to a crossover to weaker correlations at small scales n (see Fig.3e in [44]). It was also reported that with increasing the amplitude of the spikes and their concentration in the original signal the crossover scale n_x gradually moves from small to intermediate scales [44], an effect similar to the effect of Floor coarse-graining we shown in Fig.10(c,d). With increasing the partition parameter $\Delta > 1$ the difference between the values $x(i)$ of the original correlated signal and the integer (symbolic) values $\tilde{x}(i)$ in the coarse-grained signal also increases, effectively equivalent to adding random noise. Thus, as in the case of anti-correlated signals, the effect of Floor coarse-graining on the scaling of positively correlated signals is equivalent to the superposition of the scaling curve $F(n)$ of the original signal $x(i)$ with the scaling curve $F_\eta(n)$ of a white noise signal ($\alpha = 0.5$). Increasing the amplitude and standard deviation of the added white noise signal leads to an increase (a vertical shift up) in $F_\eta(n)$, and thus, a shift of the intersection (i.e., the crossover scale n_x) between $F_\eta(n)$ and $F(n)$ of the original correlated signal from small to intermediate scales n — a superposition rule first discussed in [43, 44]. However, we note that the same superposition rule leads to substantially different effects on the scaling of anti-correlated and positively correlated signals — while large, intermediate and small scales are strongly affected by increasing the coarse-graining parameter Δ for anti-correlated signals, only the small scales are slightly affected for positively correlated signals.

(ii) *Symmetry Method.* Next, we consider how symbolic coarse-graining in the magnitude based on the Symmetry method (see Section II B, Eq.6 and Fig.3) affects the scaling behavior of long-range power-law correlated signals. We find that the scaling behavior of anti-correlated signals is much strongly affected by the Symmetry coarse-graining compared to positively correlated signals.

In Fig.11a and Fig.11c we present the results of Symmetry coarse-graining for a strongly anti-correlated signal characterized by a DFA scaling exponent $\alpha = 0.1$ and a strongly correlated signal with $\alpha = 0.9$. Similarly to the Floor coarse-graining method, applying the Symmetry coarse-graining method with small values of the width of the partition interval $\Delta < 1$, the interface of the coarse-grained signal $\tilde{x}(i)$ expands along the y-axis (Fig.4b and e) leading to an increase in the standard deviation of the coarse-grained signal, and to a vertical shift up of the DFA fluctuation function $F(n)$ (Fig.11a and c). With increasing values of Δ the interface of the coarse-grained signal $\tilde{x}(i)$ shrinks, i.e., the standard deviation decreases (as shown in Fig.4c and f), and the scaling curve $F(n)$ shifts vertically down (Fig.11a). This vertical shift of scaling curves $F(n)$ is observed for both anti-correlated and positively correlated Symmetry coarse-grained signals (Fig.10a and c).

We note, that even for very large values of the Symmetry coarse-graining parameter $\Delta >> 1$ the scaling curves $F(n)$ of both anti-correlated and positively correlated signals never shift below the $F(n)$ curve of the original signal (Fig.11a and c). This is in contrast to the Floor coarse-graining method where for $\Delta > 1$ the scaling curve $F(n)$ of the coarse-grained signals (or at least a part of $F(n)$ corresponding to small scales n) shift vertically down below the scaling curve $F(n)$ of the original signal (see Fig.10a and c). For $\Delta >> 1$, both Floor and Symmetry coarse-graining method lead to practically binary symbolic series $\tilde{x}(i)$. Since the values of binary series $\tilde{x}_{\rm Floor}(i)$ produced by Floor coarse-graining are either 0 or -1 (Fig.2c and f), we can expect $\langle \tilde{x}_{\rm Floor}(i) \rangle \approx 0.5$ and the standard deviation of the coarse-grained signal $\sigma_{\rm Floor} \approx 0.5$, which is smaller than the standard deviation $\sigma = 1$ of the original signal $x(i)$, leading to a shift of the scaling curve $F(n)$ after the Floor coarse-graining below $F(n)$ of the original signal $x(i)$. In contrast, for Symmetry coarse-graining, the values of the binary series are 1 and -1 (Fig.4c and f), leading to $\langle \tilde{x}_{\rm Symmetry}(i) \rangle \approx 0$ and $\sigma_{\rm Symmetry} \approx 1$, and thus, the $F(n)$ curve of the Symmetry coarse-grained signal $\tilde{x}(i)$ never shifts below the original $F(n)$ curve.

Coarse-graining signals using the Symmetry method leads to similar crossover behaviors as we observed using the Floor method. We find that the crossover effect after Symmetry coarse-graining is more pronounced for anti-correlated signals compared to positively correlated signals. Specifically, for anti-correlated signals there is a crossover to a random behavior ($\alpha = 0.5$) at a given scale n_x, which with increasing the partition parameter Δ moves from very large scales to intermediate and small scales (see Fig.11b where the scaling curves $F(n)$ are vertically shifted for clarity). For positively correlated signals, a crossover to slightly weaker correlations at small scales appears only when applying the Symmetry method with $\Delta > 1$, and the crossover scale n_x moves from small to intermediate scales with increasing Δ (Fig.11d).

The transitions of the crossover scale n_x with increasing partition parameter Δ using the Symmetry coarse-graining method are illustrated for both anti-correlated and positively correlated coarse-grained signal in Fig.11e. Similar transition of the crossover scale n_x we also found for the Floor coarse-graining method (Fig.10e, indicating that Symmetry and Floor coarse-graining method have a similar effect on the scaling behavior of correlated signals. If we ignore the few cases when data points $x(i)$ in the original signal lie exactly on the boundaries of the partition intervals, the only difference between the Symmetry and Floor coarse-graining methods is that for values $x(i) > 0$, $\tilde{x}_{\rm Symmetry}(i) = \tilde{x}_{\rm Floor}(i) + 1$ (see Fig.1b and Fig.3b). Thus, the relative disposition of the data points $\tilde{x}(i)$ in the coarse-graining signal is similar for the Symmetry or Floor method, leading to a very similar effect on the scaling behavior of correlated signals (compare Fig.10 and Fig.11).

The DFA scaling results we obtained here for anti-correlated signals after rough coarse-graining with $\Delta \geqslant 3$ are in agreement with earlier studies of heartbeat inter-

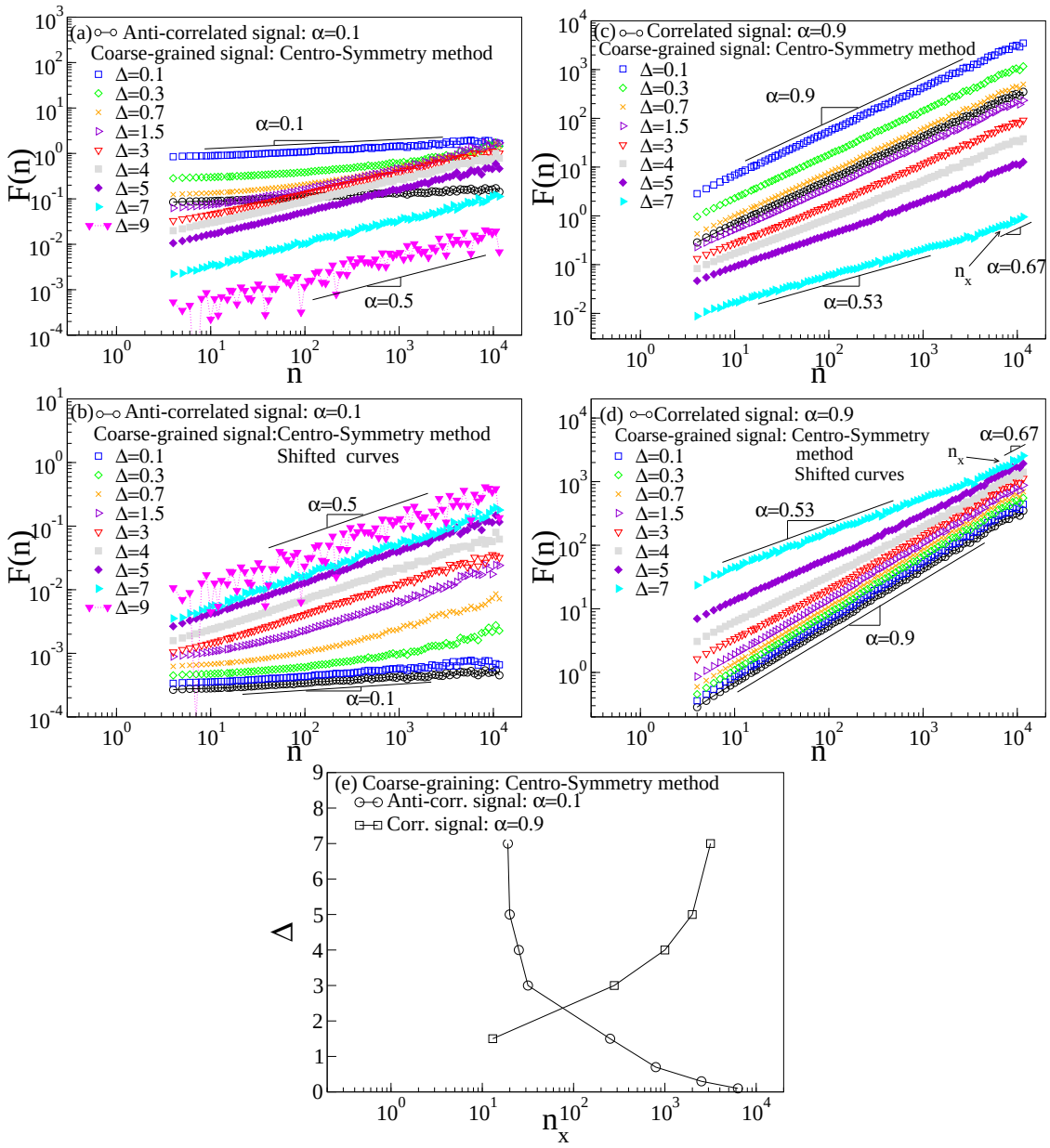

FIG. 12: Effect of the *Centro-Symmetry coarse-graining method* on the scaling behavior of long-range power-law correlated signals. Scaling curves $F(n)$ obtained using the DFA-2 method of (a) an anti-correlated signal with scaling exponent $\alpha = 0.1$, and (c) a positively correlated signal with $\alpha = 0.9$ before and after coarse-graining with different values of the partition parameter Δ. The same signals as shown in Fig.6a, d are used for the analysis. For $\Delta < 1$, the scaling curves $F(n)$ of the coarse-grained signals $\tilde{x}(i)$ shift up compared to $F(n)$ of the original signal $x(i)$ due to the expansion of the interface of $\tilde{x}(i)$ compared to $x(i)$ (shown in Fig.6b, e). With increasing $\Delta > 1$, the interface of $\tilde{x}(i)$ shrinks and $F(n)$ shifts down, similar to the Floor method (Fig.10a, c) but different from the Symmetry method (Fig.11a, c). For the anti-correlated signal in (a), the Centro-Symmetry coarse-graining leads to a crossover from anti-correlated ($\alpha = 0.1$) to random behavior ($\alpha = 0.5$) at a crossover scale n_x. For $\Delta < 1$ the crossover n_x corresponds to large scales, and moves to intermediate and small scales with increasing Δ. In contrast to anti-correlated signals, the Centro-Symmetry coarse-graining with small $\Delta < 1$ has no effect on the scaling of positively correlated signals, while for large $\Delta > 1$ there is a crossover at small scales towards random behavior ($\alpha \approx 0.5$) in contrast to the Floor and Symmetry methods. (b) and (d) show the same results as in (a) and (c) with scaling curves $F(n)$ vertically shifted to visualize the transition of the crossover n_x for different values of Δ. (e) Dependence of the crossover scale n_x on the coarse-graining parameter Δ for the anti-correlated and positively correlated signals shown in (a) and (c). Note, that n_x changes with increasing $\Delta > 3$, in contrast to the Floor and Symmetry methods where n_x stabilizes for $\Delta > 3$ (Fig.10e and Fig.11e, see also the text for explanation). We note, that the effect of the Centro-Symmetry coarse-graining method is much stronger compared to the Floor and Symmetry methods (Fig.10 and Fig.11).

val increments, where after applying the magnitude and sign decomposition method it was shown that the sign (+1 or −1) of the heartbeat increments (i.e., a binary sequence derived after "coarse-graining" of the original time series) exhibits a scaling behavior with $\alpha \simeq 0.3$ at small and intermediate time scales with a crossover to $\alpha \simeq 0.5$ at large time scales $n > 100$ [33, 35, 42].

(iii) *Centro-Symmetry Method*. The last method of coarse-graining in the magnitude we consider is the Centro-Symmetry method (see Section II B, Eq.7 and Fig.5). In Fig.12 we present the results for a strongly anti-correlated signal characterized by a DFA scaling exponent $\alpha = 0.1$ and for a positively correlated signal with $\alpha = 0.9$ (the same identical signals are used for comparison with the Floor and Symmetry coarse-graining in Fig.10 and Fig.11 respectively). We observe a vertical shift of the DFA fluctuation function $F(n)$ after Centro-Symmetry coarse-graining of both anti-correlated and positively correlated signals (Fig.12a and c), i.e., a shift up for values of the partition parameter $\Delta < 1$ and a shift down for $\Delta > 1$. This effect is very similar to the Floor coarse-graining (Fig.10a and c),

As for the Floor and Symmetry coarse-graining, for small values of Δ the Centro-Symmetry method applied to anti-correlated signal leads to a crossover at large scales to random behavior with an exponent $\alpha = 0.5$ (Fig.12b). With increasing Δ the crossover scale n_x moves to intermediate and small scales. Applied to positively correlated signals the Centro-Symmetry coarse-graining with partition parameter $\Delta < 1$ does not lead to observable changes in the scaling behavior and the scaling exponent $\alpha = 0.9$ remains unchanged across all scales n (Fig.12c and d) — similar to the Floor and Symmetry methods. In contrast, for increasing $\Delta > 1$ the Centro-Symmetry coarse-graining leads to a dramatic change from strongly correlated ($\alpha = 0.9$) towards uncorrelated ($\alpha = 0.5$) behavior with a crossover scale n_x moving from small to intermediate and large scales (Fig.12d). This effect of the Centro-Symmetry method is much stronger compared to the Floor and Symmetry methods, where for positively correlated signals the coarse-graining leads to slightly weaker correlations ($\alpha = 0.8$) only at small scales (Fig.10d and Fig.11d).

The transition of the crossover scale n_x for increasing partition parameter Δ of the Centro-Symmetry coarse-graining of correlated signals is shown in Fig.12e. For anti-correlated signals the crossover scale n_x moves from large to small scales with increasing Δ. We note that, in contrast to the Floor and Symmetry methods, n_x continues to decrease to smaller scales even when $\Delta > 3$. For correlated signals n_x moves in the opposite direction, from small to large scales with increasing $\Delta > 1$, which is in contrast to the Floor and Symmetry coarse-graining where n_x does not reach to large scales and remains stable for $\Delta > 3$ (Fig.10e and Fig.11e). The reason for this stable behavior of n_x is that for increasing $\Delta > 3$ most of the data points $\tilde{x}(i)$ become 1 and -1 for the Symmetry method and 0 and -1 for the Floor method with standard deviation of the coarse-grained signals $\sigma_{\text{Symmetry}} = 1 + \varepsilon$ and $\sigma_{\text{Floor}} = 0.5 + \varepsilon$, where the term $\varepsilon \geq 0$ is due to a few outliers $|x(i)| > \Delta$ and $\varepsilon \to 0$ for large Δ. For $\Delta > 3$ the relative contribution of ε to σ_{Symmetry} and σ_{Floor} is negligible, σ_{Symmetry} and σ_{Floor} stabilize, and thus there is no further change in the scaling curves $F(n)$ and the crossover scale n_x. In contrast, most of the data points after Centro-Symmetry coarse-graining become $\tilde{x}(i) = 0$, with a standard deviation $\sigma_{\text{Centro-Symmetry}} = \varepsilon$, where the term ε is due to a few remaining outliers $|x(i)| > \frac{1}{2}\Delta$. Because $\varepsilon \to 0$ with increasing $\Delta > 3$, $\sigma_{\text{Centro-Symmetry}}$ also continuously decreases and does not stabilize, and thus the scaling curve $F(n)$ and the crossover scale n_x continue to change as we observe in Fig.12.

B. Coarse-graining in time

In addition to coarse-graining the magnitude of a signal, we also consider how coarse-graining in time (see Section II B 2, Eq.8 and Fig.7) affects the scaling behavior of long-range power-law correlated signals. We systematically investigate the effect of time coarse-graining on both anti-correlated and positively correlated signals. In Fig.13a we present the results for a strongly anti-correlated signal with scaling exponent $\alpha = 0.1$. We find that after averaging in time the standard deviation of the signal decreases, leading to a vertical shift down of the DFA fluctuation function $F(n)$ for increasing averaging time intervals Δ. Although the averaging procedure in non-overlapping intervals Δ substantially shortens the signal (up to 50 times), the correlation properties remain practically preserved. For positively correlated signals (Fig.13b), coarse-graining also causes shift down of the scaling curve $F(n)$, however to a less extent compared to anti-correlated signals. The scaling of the positively correlated signals is well preserved after coarse-graining in time. In Fig.13c we present the dependence of scaling exponent α on the coarse-graining time intervals Δ for various correlated signals. We find that for anti-correlated signals α slightly decreases after coarse-graining, and that this decrease is more pronounced for larger Δ and for signals with stronger anti-correlations. In contrast, the scaling exponent of positively correlated signals remains practically unchanged after coarse-graining with time intervals Δ up to 100.

IV. SUMMARY

In summary, we systematically study the effect of coarse-graining in both the magnitude and time on the scaling behavior of long-range power-law anti-correlated and correlated signals. We investigate three types of coarse-graining methods in the magnitude — the Floor, the Symmetry and the Centro-Symmetry method. For coarse-graining in time, we employ a time average procedure within non-overlapping windows of fixed size.

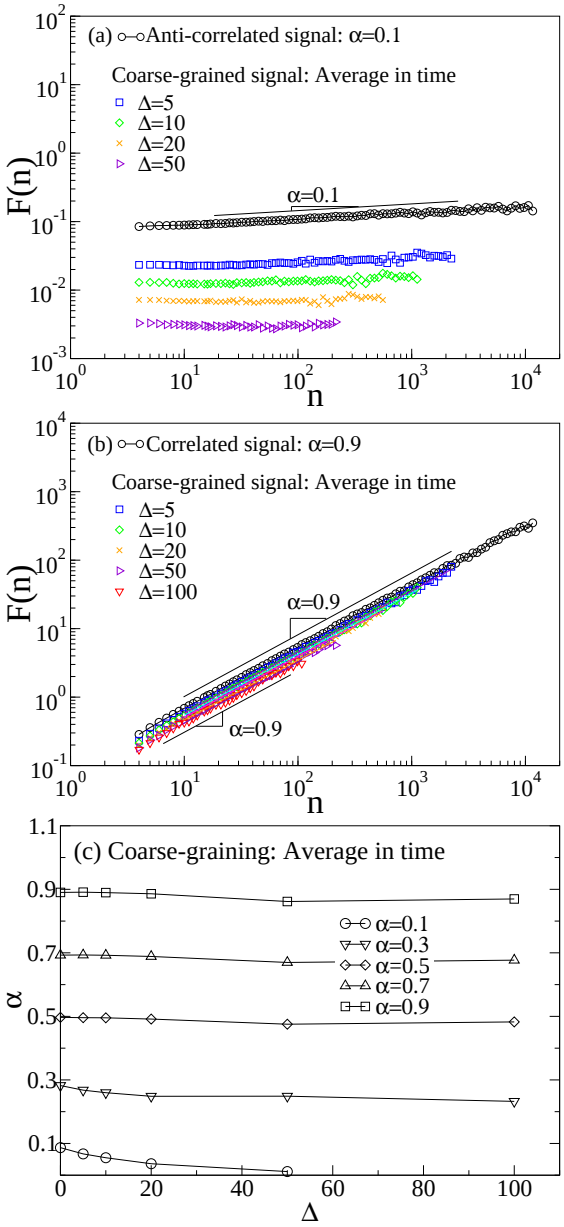

FIG. 13: Effect of *coarse-graining in time* on the scaling behavior of long-range power-law correlated signals. Scaling curves $F(n)$ obtained using the DFA-2 method of (a) an anti-correlated signal with scaling exponent $\alpha = 0.1$, and (c) a positively correlated signal with $\alpha = 0.9$ before and after coarse-graining with different values of the length of the averaging time interval Δ. The same signals as shown in Fig.8a,e are used for the analysis. The scaling curves $F(n)$ of the coarse-grained signals $\tilde{x}(i)$ are shortened due to the coarse-graining in time, and are shifted down with increasing Δ due to decreasing of the standard deviation of $\tilde{x}(i)$ compared to the standard deviation of the original signal $x(i)$. (c) Dependence of the scaling exponent α obtained for the coarse-grained signals on the size of the averaging time interval Δ. The scaling behavior of the coarse-grained signals is practically preserved for both anti-correlated and positively correlated signals. A slight decrease in α for anti-correlated signals is observed.

We find that, for both anti-correlated and positively correlated signals, all three types of coarse-graining in the magnitude lead to expanding the interface of the coarse-grained signal along the y-axis for small values of the width of the partition interval $\Delta < 1$, and to a corresponding increase and a vertical shift up of the DFA fluctuation function $F(n)$. For increasing values of Δ, the interface of the coarse-grained signals shrink and the scaling curves $F(n)$ shift vertically down.

For anti-correlated signals, all three coarse-graining methods in the magnitude have a strong and similar effect on the scaling behavior of the coarse-grained signals, leading to a crossover at scale n_x to random behavior ($\alpha = 0.5$) at large scales. With increasing values of partition parameter Δ, the crossover scale n_x moves from large to intermediate and small scales. In contrast, all three coarse-graining methods have a much weaker effect on the scaling behavior of positively correlated signals. The scaling behavior of coarse-grained positively correlated signals with partition parameter $\Delta < 1$ remains practically unchanged at both small and large scales, i.e., there is no observable crossover in the scaling curve $F(n)$. For large Δ, a crossover to slightly weaker correlations at small scales appears after coarse-graining positively correlated signals, and gradually moves to intermediate scales with increasing Δ.

For very large $\Delta > 3$, the effect of Floor and Symmetry coarse-graining on the scaling behavior and the position of the crossover stabilizes for both anti-correlated and positively correlated signals. In contrast, the effect of Centro-Symmetry coarse-graining on the scaling behavior is continuously stronger with increasing $\Delta > 3$, and the scale of the crossover n_x is continuously moving. For Centro-Symmetry coarse-graining with very large $\Delta >> 3$, the correlations of strongly correlated signals are destroyed ($\alpha \approx 0.5$) at small scales, and the correlations at large scales are weakened.

The change we observe in the scaling behavior of both anti-correlated and positively correlated signals $x(i)$ after coarse-graining in the magnitude is to some extent similar to the effect of adding noise or random spikes to long-range power-law correlated signals. With increasing the partition parameter Δ the difference between the increments of the consecutive values $x(i)$ in the original signal and the increments of the integer (symbolic) values $\tilde{x}(i)$ in the coarse-grained signal also increases, effectively equivalent to adding random noise. It was previously shown [44] that adding noise and random spikes to anti-correlated signals leads to a crossover to a random behavior at large and intermediate scales, while for positively correlated signals, a crossover to random behavior occurs at small and intermediate scales — a change in the scaling behavior which strongly resembles the effects of coarse-graining investigated here, and which can be explained by a superposition of the scaling curve $F(n)$ of the original signal and the scaling curve $F_\eta(n)$ of a white noise signal intersecting at a crossover scale n_x [43, 44].

For coarse-graining in time where data are averaged in

non-overlapping time windows, we find that the scaling curve $F(n)$ shifts down due to the decrease in the standard deviation of the coarse-grained signal, and that the scaling is practically preserved for positively correlated signals. While for anti-correlated signals there is a slight decrease in the scaling exponent.

The reported here observations are important to correctly interpret results of correlation and scaling analyses of a broad range of natural and pre-processed symbolic sequences and coarse-grained signals, and are instrumental in supporting modeling efforts of systems generating symbolic dynamics.

Acknowledgments

We thank the Brigham and Women's Hospital Biomedical Research Institute Fund, the Spanish Junta de Andalucia (Grant No. P06-FQM1858 and P07-FQM3163), the Ministry of Human Resources of P.R.China (Scientific Research Foundation for the Returned Overseas Chinese Scholars), Nanjing Normal University (Scientific Research Foundation for the Returned Overseas Chinese Scholars), and the National Natural Science Foundation of China (Grant No. 60501003) for support.

[1] R. L. Stratonovich, *Topics in the Theory of Random Noise Vol. 1* (Gordon & Breach, New York, 1981).
[2] H. E. Hurst, Trans. Am. Soc. Civ. Eng. **116**, 770 (1951).
[3] B. B. Mandelbrot, and J. R. Wallis, Water Resour. Res. **5**, 321 (1969).
[4] C.-K. Peng, S. V. Buldyrev, S. Havlin, M. Simons, H. E. Stanley, and A. L. Goldberger, Phys. Rev. E **49**, 1685 (1994).
[5] M. S. Taqqu, V. Teverovsky, and W. Willinger, Fractals **3**, 785 (1995).
[6] P. Carpena, P. Bernaola-Galván, A. V. Coronado, M. Hackenberg, and J. L. Oliver, Phys. Rev. E, **75**, 032903 (2007).
[7] G. M. Viswanathan, S. V. Buldyrev, S. Havlin, and H. E. Stanley, Biophys. J. **72**, 866 (1997)
[8] K. Ivanova, T. P. Ackerman, E. E. Clothiaux, P. Ch. Ivanov, H. E. Stanley, and M. Ausloos, J. Geophys. Res., [Atmos.] **108**, 4268 (2003).
[9] E. Koscielny-Bunde, A. Bunde, S. Havlin, H. E. Roman, Y. Goldreich, and H. J. Schellnhuber, Phys. Rev. Lett. **81**, 729 (1998).
[10] E. Koscielny-Bunde, H. E. Roman, A. Bunde, S. Havlin, and H. J. Schellnhuber, Philos. Mag. B **77**, 1331 (1998).
[11] P. Talkner, and R. O. Weber, Phys. Rev. E **62**, 150 (2000).
[12] A. Montanari, R. Rosso, and M. S. Taqqu, Water Resour. Res. **36**, (5) 1249 (2000).
[13] C. Matsoukas, S. Islam, and I. Rodriguez-Iturbe, J. Geophys. Res., [Atmos.] **105**, 29165 (2000).
[14] N. Vandewalle, and M. Ausloos, Phy. Rev. E **58**, 6832 (1998).
[15] Y. Liu, P. Gopikrishnan, P. Cizeau, M. Meyer, C.-K. Peng, and H. E. Stanley, Phys. Rev. E **60**, 1390 (1999).
[16] I. M. Janosi, B. Janecsko, and I. Kondor, Physica A **269**, 111 (1999).
[17] P. Ch. Ivanov, A. Yuen, B. Podobnik, and Y. Lee, Phys. Rev. E **69**, 056107 (2004).
[18] S. Bahar, J. W. Kantelhardt, A. Neiman, H. H. A. Rego, D. F. Russell, L. Wilkens, A. Bunde, and F. Moss, Europhys. Lett. **56**, 454 (2001).
[19] S. V. Buldyrev, A. L. Goldberger, S. Havlin, C.-K. Peng, H. E. Stanley, and M. Simons, Biophys. J. **65**, 2673 (1993).
[20] S. M. Ossadnik, S. B. Buldyrev, A. L. Goldberger, S. Havlin, R. N. Mantegna, C.-K. Peng, M. Simons, and H. E. Stanley, Biophys. J. **67**, 64 (1994).
[21] R. N. Mantegna, S. V. Buldyrev, A. L. Goldberger, S. Havlin, C.-K. Peng, M. Simons, and H. E. Stanley, Phys. Rev. Lett. **73**, 3169 (1994).
[22] R. N. Mantegna, S. V. Buldyrev, A. L. Goldberger, S. Havlin, C.-K. Peng, M. Simons, and H. E. Stanley, Phys. Rev. Lett. **76**, 1979 (1996).
[23] S. V. Buldyrev, N. V. Dokholyan, A. L. Goldberger, S. Havlin, C.-K. Peng, H. E. Stanley, and G. M. Viswanathan, Physica A **249**, 430 (1998).
[24] P. Bernaola-Galván, R. Roman-Roldan, J. L. Oliver, Phys. Rev. E **53**, 5181-5189 (1996).
[25] C.-K. Peng, S. Havlin, H. E. Stanley, and A. L. Goldberger, Chaos **5**, 82 (1995).
[26] K. K. L. Ho, G. B. Moody, C.-K. Peng, J. E. Mietus, M. G. Larson, D. Levy, and A. L. Goldberger, Circulation **96**, 842 (1997).
[27] P. Ch. Ivanov, A. Bunde, L. A. Nunes Amaral, S. Havlin, J. Fritsch-Yelle, R. M. Baevsky, H. E. Stanley, and A. L. Goldberger, Europhys. Lett. **48**, 594 (1999).
[28] S. M. Pikkujamsa, T. H. Makikallio, L. B. Sourander, I. J. Raiha, P. Puukka, J. Skytta, C.-K. Peng, A. L. Goldberger, and H. V. Huikuri, Circulation **100**, 393 (1999).
[29] T. H. Makikallio, J. Koistinen, L. Jordaens, M. P. Tulppo, N. Wood, B. Golosarsky, C.-K. Peng, A. L. Goldberger, and H. V. Huikuri, Am. J. Cardiol. **83**, 880 (1999).
[30] D. Toweill, K. Sonnenthal, B. Kimberly, S. Lai, and B. Goldstein, Crit. Care Med. **28**, 2051 (2000).
[31] A. Bunde, S. Havlin, J. W. Kantelhardt, T. Penzel, J. H. Peter, and K. Voigt, Phys. Rev. Lett. **85**, 3736 (2000).
[32] T. T. Laitio, H. V. Huikuri, E. S. H. Kentala, T. H. Makikallio, J. R. Jalonen, H. Helenius, K. Sariola-Heinonen, S. Yli-Mayry, and H. Scheinin, Anesthesiology **93**, 69 (2000).
[33] Y. Ashkenazy, P. Ch. Ivanov, S. Havlin, C.-K. Peng, A. L. Goldberger, and H. E. Stanley, Phys. Rev. Lett. **86**, 1900 (2001).
[34] P. Ch. Ivanov, L. A. N. Amaral, A. L. Goldberger, M. G. Rosenblum, H. E. Stanley, and Z. R. Struzik, Chaos **11**, 641 (2001).
[35] Y. Ashkenazy, S. Havlin, P. Ch. Ivanov, C.-K. Peng, V. Schulte-Frohlinde, and H. E. Stanley, Physica A **323**, 19 (2003).
[36] P. Ch. Ivanov, IEEE Engineering in Medicine and Biology Magazine **26**, 33 (2007).

[37] P. Ch. Ivanov, K. Hu, M. F. Hilton, S. A. Shea, and H. E. Stanley, Proc. Natl. Acad. Sci. USA **104**, 20702 (2007).
[38] D. T. Schmitt, and P. Ch. Ivanov, Am. J. Physiol.-Regul. Integr. Comp. Physiol. **293**, R1923 (2007).
[39] D. T. Schmitt, P. K. Stein, and P. Ch. Ivanov, IEEE Trans. Biomed. Eng. **56**, 1564 (2009).
[40] J. M. Hausdorff, C.-K. Peng, Z. Ladin, J. Wei and A. L. Goldberger, J. Applied Physiol. **78**, 349 (1995).
[41] Y. Ashkenazy, J. M. Hausdorff, P. Ch. Ivanov, and H. E. Stanley, Physica A **316**, 662 (2002).
[42] P. Ch. Ivanov, Q. D. Y. Ma, R. P. Bartsch, J. M. Hausdorff, L. A. N. Amaral, V. Schulte-Frohlinde, H. E. Stanley, and M. Yoneyama, Phys. Rev. E **79**, 041920 (2009).
[43] K. Hu, P. Ch. Ivanov, Z. Chen, P. Carpena, and H. E. Stanley, Phys. Rev. E **64**, 011114 (2001).
[44] Z. Chen, P. Ch. Ivanov, K. Hu, and H. E. Stanley, Phys. Rev. E **65**, 041107 (2002).
[45] Z. Chen, K. Hu, P. Carpena, P. Bernaola-Galván, H. E. Stanley, and P. Ch. Ivanov, Phys. Rev. E, **71**, 011104 (2005).
[46] Q. D. Y. Ma, R. P. Bartsch, P. Bernaola-Galván, M. Yoneyama, and P. Ch. Ivanov, arXiv:1001.3641v2 (2010).
[47] L. Xu, P. Ch. Ivanov, K. Hu, Z. Chen, A. Carbone, and H. E. Stanley, Phys. Rev. E **71**, 051101 (2005).
[48] A. Bashan, R. Bartsch, J. W. Kantelhardt, and S. Havlin, Physica A **387**, 5080 (2007).
[49] W. Li, J. Stat. Phys., **60**, 823 (1990).
[50] H. Herzel, and I. Grosse, Physica A, **216**, 518 (1995).
[51] C. J. Cellucci, A. M. Albano, and P. E. Rapp, Phys. Rev E **71**, 066208 (2005).
[52] D. Holste, I. Grosse, S. Beirer, P. Schieg and H. Herzel, Phys. Rev. E **67** 061913 (2003).
[53] R. Q. Quiroga, A. Kraskov, T. Kreuz and P. Grassberger, Phys. Rev. E **65**, 041903 (2002).
[54] B. Groisman, S. Popescu, and A. Winter, Phys. Rev. A **72**, 032317 (2005).
[55] J. M. Martinerie, A. M. Albano, A. I. Mees, and P. E. Rapp, Phys. Rev. A **45**, 7058 (1992).
[56] R. T. Wicks, S. C. Chapman, and R. O. Dendy. Phys. Rev. E **75**, 051125 (2007).
[57] J. L. Oliver, R. Roman-Roldan, J. Perez, and P. Bernaola-Galván, Bioinformatic **15** 974-979 (1999).
[58] J. L. Oliver, P. Bernaola-Galván, P. Carpena, and R. Roman-Roldan, Gene **276**, 47 (2001).
[59] J.L. Oliver, P. Carpena, R. Roman-Roldan, T. Mata-Balaguer, A. Mejias-Romero, M. Hackenberg, and P. Bernaola-Galvan, Gene **300** 117-127 (2002).
[60] W. Li, P. Bernaola-Galván, P. Carpena, and J. L. Oliver, Computational Biology and Chemistry **27** 5-10 (2003).
[61] E. B. Postnikov, A. B. Ryabov, and A. Loskutov, J. Phys. A **40**, 12033 (2007).
[62] H. A. Makse, S. Havlin, M. Schwartz, and H. E. Stanley, Phys. Rev. E **53**, 5445 (1996).